

DIETARY SUPPLEMENT REDUCES RADIATION-INDUCED MUSCLE DAMAGE

INVESTIGATING THE ROLE OF A MULTI-TARGETED DIETARY SUPPLEMENT ON
ATTENUATING RADIATION INDUCED SKELETAL MUSCLE DAMAGE

By RHEA V. VEMULA, BSc

A Thesis Submitted to the School of Graduate Studies in Partial Fulfilment of the Requirements
for the Degree Master of Medical Sciences

McMaster University © Copyright by Rhea V. Vemula, July 2025

McMaster University MASTER OF SCIENCE (2025) Hamilton, Ontario (Medical Sciences)

TITLE: Investigating The Role of a Multi-Targeted Dietary Supplement on Attenuating Radiation Induced Skeletal Muscle Damage

AUTHOR: Rhea Vaishno Vemula, BSc

SUPERVISOR: Dr. Thomas J. Hawke & Dr. David A. MacLean

NUMBER OF PAGES: xi, 56

LAY ABSTRACT

Space travel exposes astronauts to ionizing radiation (IR), which can damage muscles resulting in impaired function reduced well-being. This study explored whether a Multi-Targeted Dietary Supplement (MTDS) can aid in protecting muscle after IR exposure. Mice were fed either the control diet (CD) or a control diet containing the MTDS and then exposed to IR. CD-fed mice exposed to IR exhibited lower body weights and increased evidence of muscle damage. Muscles from the IR exposed CD mice showed increased centrally-located nuclei, a metric of muscle damage and ongoing repair. IR exposed mice on the MTDS diet did not experience these changes. These results demonstrate that the MTDS has the potential to be an aid in the protection of muscles after IR exposure, which can be useful for astronauts on extended space missions. Supported by the Canadian Space Agency

ABSTRACT

Exposure to ionizing radiation (IR) is known to negatively impact musculoskeletal health. A Multi-Targeted Dietary Supplement (MTDS) has been formulated to protect against radiation-induced cellular damage. This study investigated the efficacy of this MTDS to ameliorate IR's negative effects on skeletal muscle. Six experimental groups of ten-week-old male BALB/c mice were randomized (n=8/group) to either a control diet (CD) or the MTDS diet (MD). The MTDS was mixed into the CD, and mice were pre-fed the MD for 28 days. Each diet group was randomly divided into control (no irradiation) or an irradiated (IR) group and continued their respective diet until euthanized at day 21 or 28. IR-treated mice received 0.8 Gy fractions (day 0 and 14 or day 0, 7 and 14) for a cumulative dosage of 1.6 or 2.4 Gy, respectively. Tibialis anterior (TA), quadriceps, gastrocnemius and plantaris (GP), and soleus muscles were collected. Body weights remained unchanged at 1.6 Gy, while a reduction was observed at 2.4 Gy in the IR+CD group compared to the IR+MTDS group. The relative TA and GP muscle/body weight ratios were elevated in IR+CD groups, whereas the MD maintained lower muscle/body weight ratios. Cross-sectional area and min Feret values in the IR+CD were larger compared to control and the IR+MD groups demonstrating that the MTDS was protective against radiation-induced edema. Centrally-located nuclei (per mm²) in the IR+CD group were significantly elevated in both the TA and GP compared to control and the IR+MTDS group. Macrophage F4/80 staining showed a significant increase in macrophages within muscle fibers in the IR+CD groups, which was blunted by the MD. These results demonstrate that IR exposure leads to long-term negative changes on skeletal muscle and the MTDS attenuated these effects, positioning it as a potential therapeutic approach to IR exposure.

Supported by the Canadian Space Agency.

ACKNOWLEDGEMENTS

I would first like to thank my wonderful supervisors, Dave and Tom, for their unwavering support, guidance and mentorship throughout my Master's journey. Coming into the lab without any prior wet lab experience, I am deeply grateful for the patience and dedication you both showed in teaching me the skills required for this project. You never failed to answer my endless questions and your encouragement and belief in me has been invaluable. I am so thankful to have had the opportunity to work under you and will cherish the relationships and experiences I have gained along the way.

The biggest thank you to all my amazing lab members for your support for my numerous harvests, laughter, and endless memories. A special thank you to Irena, who became my pillar of support and guiding voice during the last few months of my thesis. Thank you, Meghan for being my mentor, helping me with harvests, and providing me advice with all things in life. Alex and Anika, in the shortest time we have become really good friends, and I cherish all the memories we made both in the lab and outside, from singing, harvest playlists, and Jenga during lunch to drinks at Fairweather. Thank you to all my past and present undergrads and lab members who helped with my project. Thank you to my friends from the Steinberg lab, especially Fiorella and Therese, who have supported me with great vibes and laughter which brightened the toughest days.

Zara, Valerii, and Cassandra, thank you for always being by my side during these last two years and beyond. The coffees dropped off, late night study sessions, and kind words of support were felt much more deeply than you could have ever imagined. Zara thank you for being my constant study buddy and cheerleader, there could be no one else I would want to do my master's side by side with.

Thank you to my committee members, Dr. Irena Rebalka and Dr. Martin Gibala for your advice and insight was greatly appreciated and made my project better.

Thank you to all the McMaster animal facility staff who advocated for the study and took care of my animals and introduced me to furry friends.

Lastly, my family, thank you Mummy and Papa for always teaching me to dream big, believing in me, and listening to all my presentations I have ever given since I was a child. You both are the reason I work hard and strive to be my best. I dedicate this Master's to you.

TABLE OF CONTENTS

LAY ABSTRACT	iii
ABSTRACT.....	iv
ACKNOWLEDGEMENTS.....	v
TABLE OF CONTENTS.....	vii
LIST OF FIGURES AND TABLES	ix
LIST OF ABBREVIATIONS AND SYMBOLS	x
DECLARATION OF ACADEMIC ACHIEVEMENT.....	xi
LITERATURE REVIEW	1
Chapter 1: Space Travel.....	1
1.1 Introduction to Space travel.....	1
1.2 Space Radiation	2
1.3 Types of IR Exposure.....	3
Chapter 2: Skeletal Muscle Overview	5
2.1 Muscle Structure and Function	5
2.2 Muscle Regeneration and Regulation	6
Chapter 3: Radiation Mediated Alterations to Skeletal Muscle.....	8
3.1 Inhibition of Muscle Satellite Cells	8
3.2 Altered Muscle Morphology	9
3.3 Radiation Induced Muscle Fibrosis	11
Chapter 4: Interventions.....	12
4.1 Current Interventions - Exercise and Shielding.....	12
4.2 Multi-Targeted Dietary Supplement	13
PURPOSE	15
METHODS	16

RESULTS.....	23
DISCUSSION	41
FUTURE DIRECTIONS	48
REFERENCES	50

LIST OF FIGURES AND TABLES

Figures from Literature Review

Figure 1.	Graphical display of the types of space radiation and effects from NASA.	4
Figure 2.	Visual representation of the experimental timeline.	19

Figures from Results

Figure 3.	Changes in body weights at day 21 and day 28 following exposure to 1.6 or 2.4 Gy of IR.	24
Figure 4.	Tibialis anterior (TA) muscle/body weight ratios (%) at day 21 and day 28 following exposure to 1.6 or 2.4 Gy of IR.	26
Figure 5.	Quadricep muscle/body weight ratios (%) at day 21 and day 28 following exposure to 1.6 or 2.4 Gy of IR.	28
Figure 6.	Gastrocnemius and plantaris (GP) muscle/body weight ratios (%) at day 21 and day 28 following exposure to 1.6 or 2.4 Gy of IR.	30
Figure 7.	Soleus muscle/body weight ratios (%) at day 21 and day 28 following exposure to 1.6 or 2.4 Gy of IR.	32
Figure 8.	TA cross-sectional area and min Feret diameter at day 21 and day 28 following exposure to 1.6 or 2.4 Gy of IR.	34
Figure 9.	Number of centrally-located nuclei relative to surface area in the TA muscle at day 21 and day 28 following exposure to 1.6 or 2.4 Gy of IR.	36
Figure 10.	Number of centrally-located nuclei relative to surface area in the GP muscle at day 21 and day 28 following exposure to 1.6 or 2.4 Gy of IR.	38
Figure 11.	Percentage of intrafiber macrophages in the TA muscle at day 21 and day 28 following exposure to 1.6 or 2.4 Gy of IR.	40

LIST OF ABBREVIATIONS AND SYMBOLS

IR	Ionizing Radiation
GCRs	Galactic Cosmic Rays
SPEs	Solar Partial Events
Gy	Gray
Il-6	Interlukin-6
Il- β	Interleukin-beta
Il- γ	Interleukin-gamma
TNF- β	Tumor Necrosis Factor Beta
G ₁ /S	Growth One/Synthesis phase
G ₂ /M	Growth Two/Mitosis
TA	Tibialis Anterior
SDH	Succinate dehydrogenase
CSA	Cross-sectional Area
Il-1	Interleukin-1
MyF5	Myogenic Factor 5
MyoD	Myogenic Determining Factor
MyoG	Myogenin
MTDS	Multi-Targeted Dietary Supplement
Tg	Transgenic Growth Hormone
8-OHdG	8-hydroxy-2'-deoxyguanosine
GP	Gastrocnemius and Plantaris
OCT	Optimal Cutting Temperature Compound
H&E	Hematoxylin and Eosin
PFA	Paraformaldehyde
PBS	Phosphate-Buffered Saline
NGS	Normal Goat Serum
DAPI	4',6-diamidino-2-phenylindole

DECLARATION OF ACADEMIC ACHIEVEMENT

Rhea Vemula was the primary author and responsible for majority of the data collection and analysis. Dr. David MacLean was responsible for conceptualization and study design. Both Dr. David MacLean and Dr. Thomas Hawke were responsible for experimental planning and assisted with analysis.

LITERATURE REVIEW

Chapter 1: Space Travel

1.1 Introduction to Space travel

Space travel has been a topic of fascination for decades and through it humanity has been able to explore new frontiers and understand our place in the universe. Despite the scientific advances provided by space exploration, space radiation presents unique challenges to the human body. These challenges are a primary limitation in furthering space travel, and it is imperative that research is conducted to minimize these challenges as space exploration is essential in discovering the origins of life, learning about our own planet, and potentially even furthering human survival.

Future long-duration space missions will require prolonged exposure to the stressors of space flight. For example, a return trip to Mars would last approximately two years, roughly half of which would be spent in a zero-gravity spacecraft. During this journey, the human body would be exposed to chronic micro- or partial gravity alongside volatile space radiation¹⁻⁴, known as ionizing radiation (IR)⁵. Due to IR and unweighting caused by altered gravity, there are numerous physiological changes to the human body during spaceflight. For example, the cephalic fluid shift caused by microgravity can affect visual acuity and induce profound cardiovascular changes and splanchnic pooling^{6,7}. These changes can extend to the musculoskeletal system, which faces significant challenges in the space environment. A main point of concern during spaceflight is the loss of muscle mass, and a subsequent decrease in strength, mobility, and functionality. It is estimated that astronauts can experience muscle loss of

10-20% on short-term missions⁸. However, during long term missions, loss of muscle is much more exacerbated^{9,10}. A substantial loss of skeletal muscle would have significant impact on both our metabolic and physical well-being as this tissue comprises 40% of the total body mass¹¹. Overall, the detrimental impacts of space travel on muscle results in loss of functional strength required for both mission critical activities but also can impact the overall quality of life if adequate muscle recovery is not achieved when astronauts return back to Earth.

Although there is an abundance of literature on how space travel impacts the musculoskeletal system, studies have typically focused on the impacts of weightlessness on skeletal muscle health and IR on bone health. Very few studies have focused on both dual interventions and even fewer have focused on understanding low dose IR exposure on skeletal muscle. This literature review hopes to provide a summary of the research on how spaceflight induced IR affects the musculoskeletal system, focusing specifically on skeletal muscle and will highlight areas where further investigation is needed further.

1.2 Space Radiation

The earth is protected from the harmful effects of space radiation by the ozone layer and the Van Allen Belts, a protective magnetic field composed of high energy particles that originate from the sun¹². Astronauts traveling beyond the Van Allen Belts are exposed to IR which can have various damaging impacts on their health and quality of life even after returning to earth. Space radiation is mainly comprised of IR, which is composed of gamma and x-rays, along with highly charged protons, neutrons, and beta particles¹³.

Ionizing radiation exposure occurs mostly through galactic cosmic radiation (GCRs), solar particle events (SPEs), and a smaller amount through intravehicular radiation¹⁴ (Fig. 1).

GCR is emitted as clouds of high-energy protons and alpha particles, which is thought to be originated from supernovas. This type of radiation will comprise a major portion of the radiation absorbed by astronauts¹⁴. SPEs are released by the sun during solar storms or solar flares¹⁴ and these can occur suddenly, over a short period of time and can cause intense radiation storms. Astronauts who may be conducting extravehicular activity at the time of a SPE can receive a lethal dose of radiation of up to 2 Gray (Gy)^{15, 16}. SPEs can sometimes be predicted due to the activity of an SPE being proportional to sunspot activity, which follows an eleven-year solar cycle¹⁴. However there have been occurrences of SPE activity outside of high sunspot activity, and as a result forecasting alone is not a perfect measure of predicting radiation exposure. Intravehicular radiation is produced by the interaction of SPE protons and heavy-charged GCR particles with the spacecraft itself. This type of interaction produces secondary particles through nuclear fission reactions such as protons, alpha and beta particles, gamma and x-rays, neutrons, and heavy-charged particles¹⁴. In summary, while the Earth's natural magnetic field and ozone layer shield humans from the harmful effects of IR, astronauts venturing on space missions are exposed to various different sources of IR which are sometimes unpredictable. As such IR presents a significant risk to astronaut health both in space and after return to Earth.

1.3 Types of IR Exposure

Depending on the amount of radiation and the duration of radiation exposure there are two categories of impacts. Acute impacts of radiation occurs when a large dose of radiation is absorbed in a short period of time, often minutes to hours, leading to nausea, vomiting, fatigue, and central nervous system diseases which can lead to lasting motor and behavioural impairments^{14,17,18}. Chronic exposure to radiation is when smaller radiation doses are

accumulated over decades, this is most relevant to astronauts on space missions. This type of exposure results in an increased risk of cancer, cardiovascular dysfunction and spaceflight associated neuro-ocular syndrome (SANS)^{17,18}. Currently there is an abundance of literature on how IR effects the various systems in the human body, such as the brain, heart, gastrointestinal tract and immune system^{3,18–25}. However, there is very limited knowledge on the effects of chronic exposure to radiation on skeletal muscle which is the focus of this thesis.

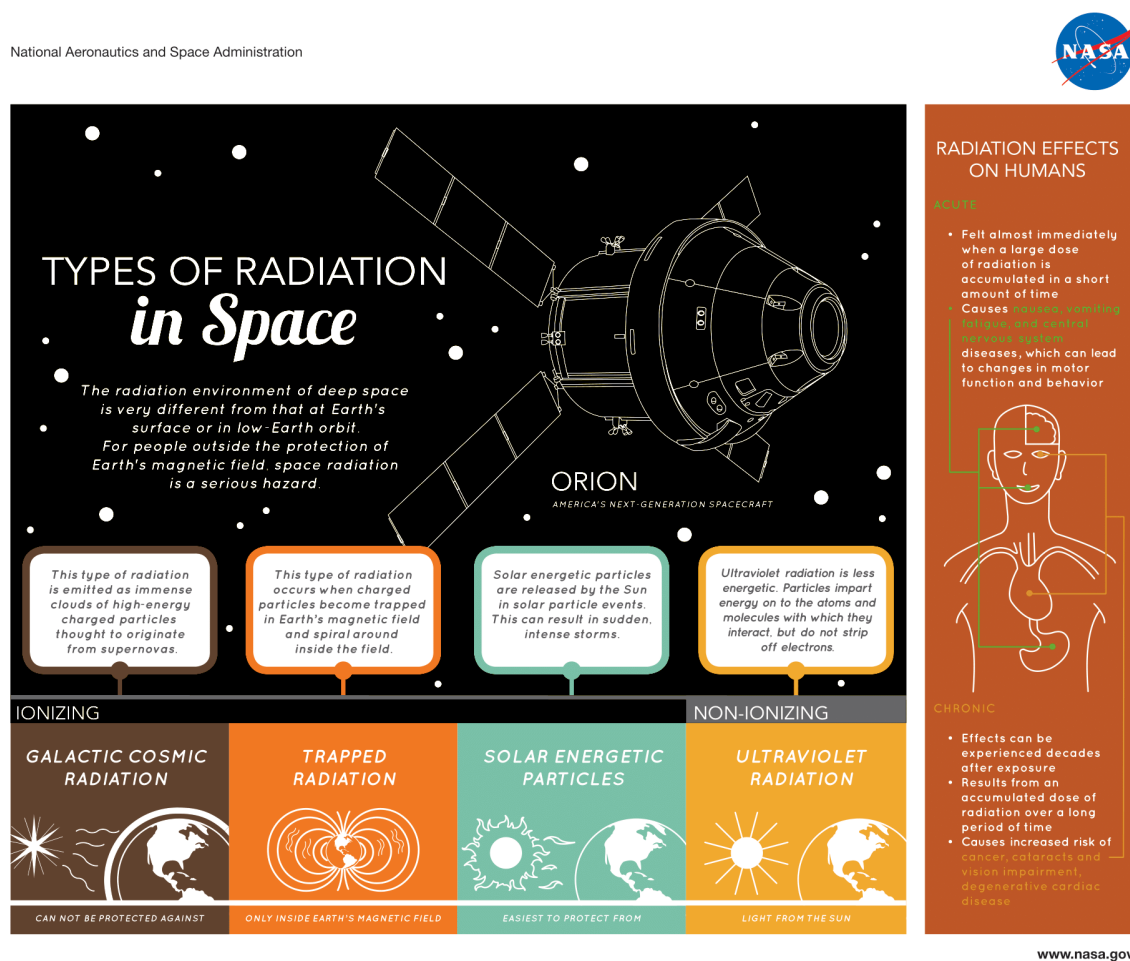


Figure 1. Graphical display of the types of space radiation and effects from NASA.

Chapter 2: Skeletal Muscle Overview

2.1 Muscle Structure and Function

The musculoskeletal system is the largest organ system within the human body (by mass) and is the foundation of human movement and function²⁶. It is comprised of bones for structural support, cartilage that ensures smooth joint movement, ligaments and tendons that connect muscles to bone, and lastly muscles, which are the focus of this thesis. Muscles generate the force necessary for movement^{26,27} and essential for vital tasks such as maintaining posture, balance, and overall movement^{28,29}. There are three types of muscle tissue, cardiac, smooth, and skeletal muscle. The focus of this thesis will be on skeletal muscle which is composed of bundles of muscle fibers called myofibers which contain many myofibrils. Each myofiber represents a muscle cell, which is surrounded by the sarcolemma, a membrane, which contains the sarcoplasm the cytoplasm of muscle cells¹¹. The functional unit of a myofibril is called a sarcomere, which is composed of actin (thin filaments) and myosin (thick filaments) that slide past each other during muscle contraction, generating the force required for muscle contraction and effectively shortening the sarcomere^{30,31}. The repeating arrangement of sarcomeres gives skeletal muscle fibers their striated appearance³¹. The contractions produced by the sarcomeres for generating movement is known as the sliding filament theory³⁰, more can be read about this theory in a review published by Powers et al, 2024.

Skeletal muscle fibers can be classified into groups based on their contraction speed and metabolic phenotype. There are two main types of muscle, slow-twitch and fast-twitch fibers, each of which can be further divided into specific fiber types. Slow-twitch fibers (Type I) appear bright red and are composed of high myoglobin and mitochondrial content, and are characterized by a slow contraction speed, high oxidative capacity, resistant to fatigue and dense

capillarization³². Fast-twitch (Type II) fibers appear to be whiter, have low myoglobin and mitochondrial content, and are known to rely mainly on glycolytic pathways. Type IIA fibers are classified as fast oxidative, have intermediate amount of myoglobin, mitochondria, and capillarization, and are moderately fatigue resistant^{32,33}. Type IIX, known as hybrid fibers, are fast oxidative fibers with a fast contraction speed, however, are myoglobin and mitochondria poor, quickly fatigued and have the least amount of capillarization³². Type IIB fibers, primarily found in rodents, have a fast contraction speed, however slower than Type IIX, have very low oxidative capacity, contain low numbers of mitochondria, and are highly glycolytic. Human skeletal muscle primary consists of Type I, IIA, and IIX fibers, with few Type IIB fibers^{34,35}. Mouse species contain low numbers of Type I fibers, found primarily in the soleus, and are mostly composed of Type IIX and IIB fibers. Despite these differences, mouse models remain highly valuable for studying skeletal muscle biology as they are still able to undergo fiber type shifts, regeneration, and adaptations similar to those seen in human skeletal muscle. The different muscle fiber types are essential in allowing the body to adapt to a wide range of physical activities and demands³⁵. Furthermore, the plastic nature of muscle, allows the body to change the composition of the muscle fibers in adaptation to exercise training, injury, or in the context of spaceflight, inflammation, and weightlessness^{36–39}.

2.2 Muscle Regeneration and Regulation

The plasticity of skeletal muscle is regulated by a host of different cell types such as satellite cells, immune cells, endothelial cells, and fibro/adipogenic progenitors to name a few⁴⁰. For the purpose of this thesis satellite cells and macrophages are of interest in the context of muscle repair following exposure to injury. Satellite cells are also known as muscle stem cells.

These cells normally exist in a quiescent state, situated between the sarcolemma and the surrounding basal lamina⁴¹. Upon injury, stress, or intense physical activity, these cells are activated to respond to the physical or chemical damage caused to the myofiber. Once activated, they begin to proliferate, differentiate, and ultimately fuse with existing muscle fibers or with each other to form new fibers^{41,42}. This process is essential for repairing damaged muscle tissue caused by injury, but also for muscle growth and adaptation in response to exercise⁴². The ability of muscles to regenerate makes them highly adaptable, ensuring that they can recover from injury and maintain function. However, in cases such as muscular dystrophy where there is continuous repair required of muscle, this can lead to a diminishing pool of satellite cells due to over activation^{40,43}. It is hypothesized this pattern can be observed not only in muscular dystrophies but also due to long term IR exposure⁴⁴⁻⁴⁶.

Macrophages also play a key role in muscle repair and regeneration. Macrophages appear in two main forms, pro-inflammatory M1 macrophages, and anti-inflammatory M2 macrophages⁴⁷. Roughly 48 hrs after injury activation of M1 macrophages peak and secrete pro-inflammatory cytokines such as interleukin-6 (IL-6), IL-1 β , interferon- γ , and Tumor Necrosis Factor alpha (TNF- α)^{47,48}. These cytokines promote proliferation of myogenic precursor cells while inhibiting satellite cell differentiation. Furthermore, M1 macrophages recognize damaged muscle fibers and phagocytose the damaged tissue. Around the 4-day mark, M2 macrophages become active and support myogenesis and regeneration by secreting high levels of Insulin-like Growth Factor 1 to promote satellite cell proliferation and lower levels of Growth Differentiation Factor 3, and TNF β which promote myocyte differentiation^{47,49}. Most macrophages disappear after recovery and regeneration of healthy muscle fibers, however few macrophages remain, as resident macrophages⁵⁰, underneath the basal lamina to promote normal muscle homeostasis and

can be activated to increase recruitment of M1 macrophages following injury. As such macrophages are essential in muscle repair and maintenance and their role becomes important post IR induced skeletal muscle damage.

Chapter 3: Radiation Mediated Alterations to Skeletal Muscle

3.1 Inhibition of Muscle Satellite Cells

One of the underlying mechanisms for muscle atrophy is the insufficient activation of satellite cells, which can stunt repair and regeneration of damaged muscle fibres, leading to increased autophagy and apoptosis^{40,43}. Using earth-based IR sources, studies have explored how high-dose radiation can impact skeletal muscle satellite cells *in vitro*. Exposure to radiation of 4, 6 and 8 Gy on human myoblast cell culture derived from satellite cells has been shown to inhibit proliferation and increase stress factors such as lactate dehydrogenase, IL-6 and heat shock proteins⁴⁶. Satellite cells in cell culture, collected from the hindlimb muscle groups of female Sprague-Dawley rats were exposed to 2 or 5 Gy of gamma radiation, which resulted in a reduction in proliferation of 50% to 70%, respectively⁵¹. Furthermore, reduction in satellite cell proliferation was coupled with an increase in apoptosis and cell cycle arrest at both G₁/S (growth one and synthesis phase) and G₂/M (growth two and mitosis) check points⁵¹. This observation strongly suggests that radiation negatively impacts satellite cell numbers.

An *in vivo* study completed by Masuda et al. 2015⁴⁴, investigated the effects of varying doses of 2, 10, 50, and 250 mGy/day of whole-body gamma irradiation on C57BL/6 male mice over 30 days to determine the effects of very low to high exposures. At moderate (50 mGy/day) and high doses (250 mGy/day), there was a significant reduction in the number of myonuclei and Pax7-

positive satellite cells immediately after radiation exposure, demonstrating a negative impact on the regenerative capacity of muscle tissue⁴⁴. Interestingly, self-renewal of satellite cells was upregulated at moderate and high doses, suggesting that radiation-induced stress might promote the self-renewal of satellite cells to maintain a stem cell pool, despite reduced proliferation capacity. Three months after IR, the number of satellite cells returned to normal levels in the moderate and high doses, however, very low dose radiation (2 and 10 mGy/day) slightly impaired the proliferation capacity of satellite cells, indicating these doses may have long-term impacts on muscle regeneration.

Overall, research suggests that radiation exposure both acute and chronic negatively affect satellite cell function, compromising the muscle's ability to repair and regenerate, and leading to long-term deterioration in muscle health^{44-46,52,53}.

3.2 Altered Muscle Morphology

Very few studies have been conducted examining the changes in muscle fiber size, and composition following exposure to IR doses that are relevant to spaceflight. However, one study that was conducted by Hardee et al., 2014⁵⁴ on the hindlimbs of female C57BL/6 mice used two different radiation exposures where the first consisted of 4 fractionated doses of 4 Gy and the second of a single dose of 16 Gy. Although these doses were much higher than what astronauts would be exposed to, this research demonstrates muscle fiber type specific changes, which may be translatable to lower doses of IR exposure. The researchers observed that two weeks after IR exposure there were no differences between the irradiated and control tibialis anterior (TA) and gastrocnemius weights. However, it was observed that exposure to a single dose of 16 Gy decreased the total muscle protein and RNA content in the gastrocnemius, however, the

fractionated dose of 4x4 Gy did not have the same effect. This indicates that higher radiation exposure had a more pronounced impact on muscle protein and RNA levels⁵⁴. Both 16 Gy and 4x4 Gy increased the incidence of centrally-located nuclei within TA muscle fibers compared to control, indicating activation of muscle regeneration processes. Furthermore both 16 Gy and 4x4 Gy reduced the mean cross-sectional area (CSA) in the TA of type IIB myofibers (fast-twitch muscle fibers), however, only 16 Gy decreased the CSA of type IIA myofibers (intermediate fast-twitch fibers). This indicates that the higher dose affected both fiber types more extensively⁵⁴. Both treatments reduced the frequency and size of muscle fibers exhibiting low succinate dehydrogenase activity (SDH), which are normally Type IIB fibers, which is indicative of a decrease in oxidative capacity. These findings suggest that larger doses of IR delivered at a single instance cause more extensive muscle damage and remodeling, which were present even 2 weeks after IR exposure.

Another study investigated the effects of low dose exposure to GCRs by exposing male C57BL/6 mice to 0.24 - 0.31 Gy of GCRs⁵⁵. Galactic Cosmic Rays were simulated at Brookhaven National Laboratory using a Booster Accelerator. They showed that there were no differences in triceps brachii weights between the control and irradiated groups 9 weeks after exposure to IR. The mean CSA of muscle fibers of irradiated mice had slightly lower means compared control mice, although not significant⁵⁵. After classification of fiber types as small ($CSA < 1,700\mu m^2$) or larger fibers ($CSA > 3,000\mu m^2$) found that irradiated mice expressed significantly fewer smaller fibers⁵⁵. Furthermore, this study also noticed significantly higher number of centrally-located nuclei in the irradiated group compared to control suggesting that IR exposure resulted in muscle remodelling and regeneration.

These two studies analyzed different muscles, used different IR dose delivery modes, and had different time point for tissue collection. Despite this both studies had similarities in observing increases in centrally-located nuclei and fiber type shifts indicating that skeletal muscle is highly sensitive to IR which result in muscle damage, but not necessary a loss in muscle mass.

3.3 Radiation Induced Muscle Fibrosis

One of the later impacts of radiation exposure on muscle is the formation of fibrosis. Muscle fibrosis is the accumulation of primary collagen, followed by elastin, glycoproteins and proteoglycans⁵⁶ and when combined reduces the muscles' ability to contract and reduces its ability to regenerate and function, ultimately resulting in physical manifestations such as muscle fatigue. Radiation-induced fibrosis, in the rat model is promoted by TNF α , interleukin one (IL-1), IL-6, and TGF- β 1. When muscle is damaged, satellite cells are recruited and express myogenic factor 5 (MyF5) and proliferate and undergo myogenic differentiation. They then express myogenic determining factor (MyoD), followed by myogenin (MyoG), which promotes the repair of damaged fibers through the fusion of myoblasts. Along with the increase in cytokines and activation of other intracellular pathways, there is also an activation of fibroblasts and epithelial mesenchymal to start the transition of vascular endothelial cells to form myofibroblasts. These myofibroblasts form new connections and provide structure to muscle tissue. Once the repair is complete the pathway is turned off, however sustained activation of this pathway leads to an increase of myofibroblasts which promotes collagen secretion, leading to fibrosis⁵⁶. It was found that in rat models radiation doses starting with 65 Gy and higher all developed fibrosis and the severity level was proportional to the dosage of radiation⁵⁶. The

radiation dosages used on these rats was substantial, and it is unlikely that such large doses would be experienced during spaceflight, however this study underlines the importance of understanding radiation mediated muscle fibrosis in the context of long duration space travel.

Chapter 4: Interventions

4.1 Current Interventions - Exercise and Shielding

The current approach to mitigating the loss of muscle mass and fibres involves exercise and shielding. Exercise has many positive effects on skeletal muscle such as promoting the upregulation of protective heat shock proteins⁵⁷, increasing protein turnover^{57,58}, and activates satellite cell activity which aid in muscle regeneration and hypertrophy^{40,43,59}. While exercise is important in maintaining skeletal muscle mass, studies which have investigated space flight conditions have shown exercise is not wholly protective against space flight induced muscle atrophy^{60–63}. Furthermore, exercising in space is quite difficult and adds significant payload to the ship as specialized equipment must be used to create resistance in a weightless environment⁶³.

Shielding is a barrier between astronauts and IR, which is provided by the spacecraft in the habitation module. Some of the types of material used to shield on earth consist of lead, liquid hydrogen, and carbon fiber reinforced plastic⁶⁴. Finding a material that has low density, high mechanical strength and able to resist the penetration of IR is very difficult. Currently aluminum and carbon fiber reinforced plastics^{64,65} are the standard for spaceflights, however, research has shown that these materials are not wholly protective against all IR types. Shielding against GCRs is only partially affective, and this becomes a pronounced issue during long term

space travel as GCRs are one of the most common types of IR^{63–65}. These limitations underscore the need for adjuvant strategies to safeguard astronaut health during prolonged space missions.

4.2 Multi-Targeted Dietary Supplement

A potential strategy to mitigate radiation-induced muscle damage is a nutritional supplement that could be taken prior to and during the space mission. Recent studies from our collaborators identified a Multi-Targeted Dietary Supplement (MTDS) as a novel and promising approach to support and protect molecular pathways from damage associated with radiation conditions encountered in space^{66–70}. Although the exact formulation of the MTDS is proprietary it is comprised of various vitamin, minerals and plant and animal extracts⁶⁷. Each of the components in the supplement have been studied to be effective in reducing inflammation, insulin resistance and aid in mitochondrial regulation.

The MTDS has also been shown to improve lifespan⁶⁷ and preserve cognitive function in aging mice^{66,69,70}. Studies used transgenic growth hormone (Tg) mice as a model to display accelerated ageing and elevated sensitivity to oxidative stress and radiation, making them a suitable model for detecting the protective effects of the dietary supplement. One study showed an overall increase of 28% in longevity and life span in supplemented Tg mice, that were started on the supplement at 2 months of age and continued to receive it for their entire lifespan, compared to unsupplemented Tg mice⁶⁷. Lastly, mice who received the supplement daily for nearly two years found that the MTDS not only abolished age-related cognitive decline in Tg mice with elevated free radical processes but also allowed older treated mice to learn a cued spatial maze, indicating a preservation of cognitive function⁶⁹.

The MTDS had been tested for its efficacy against oxidative damage from IR in the form of gamma rays from a cesium-137 source⁶⁸. In this specific study researchers focused on damage produced by free radicals which lead to double strand breaks, which was measured through the marker γ H2AX and oxidative damage through the marker 8-OHdG in the chromosomes arrested in metaphase of bone marrow cells collected from mice exposed to radiation. Tg mice were paired with their normal siblings and at three months both groups were given the liquid form of the MTDS soaked on a piece of bagel. At seven months the mice were exposed to 2 Gy of gamma radiation. The results indicated that compared to the unsupplemented Tg and control groups, the supplement groups expressed six-fold lower levels of radiation induced chromosomal aberrations and lower levels of γ H2AX and 8-OHdG. This study shows that the MTDS is effective at diminishing oxidative stress in bone marrow cells following exposure to gamma radiation.

The experimental findings supporting the effectiveness of the MTDS in diminishing oxidative stress following IR exposure makes it an attractive potential intervention for astronauts in space. However, since the maximum radiation exposure dose for astronauts is 1Gy, the effectiveness of the MTDS in protecting skeletal muscle tissue at lower radiation doses that are relevant to space flight requires further investigation.

PURPOSE

The purpose of this research is to investigate the effects of IR on skeletal muscle morphology and to assess the efficacy of the MTDS in protecting skeletal muscle from the deleterious effects of IR.

Objective 1: To evaluate changes in body and muscle weights following exposure to spaceflight relevant (cumulative) doses of IR, 1.6 or 2.4 Gy, in mice fed either the MTDS diet or control diet.

Objective 2: Assess changes in muscle morphology by analysing changes in the myofiber CSA and min Feret values to determine the effects of IR and the role of the MTDS in protecting skeletal muscle.

Objective 3: Investigate metrics of muscle damage markers by quantifying centrally-located nuclei and macrophage content within skeletal muscle after exposure to IR in mice fed the MTDS and control diets.

METHODS

Animal model

Ten-week-old male BALB/c mice from Charles River Laboratories were delivered to McMaster's Animal Care Facility, where animals were acclimated for one week prior to the study. All experimental procedures were approved by McMaster's Animal Research Ethics Board. The mice were randomly divided into groups of eight with two extra mice in the radiation groups in case of attrition.

Radiation Procedure

Exposure to Ionizing Radiation (IR) was accomplished by exposing mice to gamma ray beams from a Cesium- 137 source (Gammacell 3000-unit, Best Theratronics Ltd, Ottawa, Canada). The mice were placed inside a plastic container of 4.5 inches in diameter, which is designed to fit 2 mice. These containers can be stacked into a lead, cylindrical container to allow the irradiation of 4 mice at a time (3 containers total, top container held 2 mice, middle container remained empty, and bottom container held 2 mice). The middle container was kept empty as it receives a lower dose compared to the top two containers. The mice were then exposed to a dosage of 0.8 Gy during each radiation day, resulting in a cumulative dosage of 1.6 or 2.4 Gy. Radiation days were days 0 and 14 or days 0, 7 and 14 for 1.6 or 2.4 Gy, respectively.

Dietary Supplement

The exact formulation of the MTDS is proprietary however it contains plant extracts, vitamins, minerals, and fish oil⁶⁶. The MTDS was mixed into the mouse chow pellets and based on the average consumption of 4 g per day. Assuming 4g/day food consumption, each mouse will

consume 35 mg of the MTDS and 10 mg of fish oil. Experimental groups which were fed the supplement underwent a 28-day pre-feeding and remained on their respective diet throughout the study. Additionally, mice on the MTDS diet were weighed each time their food was replenished, and individual food intake was recorded throughout the study to ensure adequate supplement consumption. The supplement had been designed to be isocaloric to the control diet to ensure calories were not a variable in study design.

Experimental Design

This masters project is a smaller portion of a much larger project, which also includes a hindlimb suspension component. As a result, the timelines chosen are reflective of the larger project to align with the hindlimb suspension and recovery component.

There were six experimental groups which underwent the following treatments:

True Control Group: Mice in this group did not receive any treatments or interventions and serve as a control for all experimental groups, harvested on day 0. The total number of animals for this group was 8.

The MTDS Control Group: These mice helped to understand how the MTDS impacts tissue in the absence of stressors. Mice in the MTDS groups followed a 28-day pre-treatment protocol and continued to consume the supplement for another 28 days with groups being sacrificed following pre-treatment, day 0, and then day 21 and day 28. Eight animals were scarified at each time point and the total sample size for this population was 24 animals.

Ionizing Radiation (IR) 2.4Gy Control Group: These mice were used to study the effects of IR on tissues. Mice were irradiated on days 0, 7, and 14 and then one group was sacrificed at day 21

and another at day 28. Eight animals were sacrificed at the first time point, and 8 animals at the second, for a total sample size of 16.

IR 1.6Gy Control Group: Mice were irradiated on days 0 and 14 and then one group was sacrificed at day 21 and another at day 28, for a total sample size of 16.

The MTDS and Radiation Groups (1.6Gy & 2.4Gy): These mice consumed the MTDS for 28 days (pre-treatment) similar to the MTDS control group, followed by another 28 days where they either received radiation on days 0, 7, and 14 cumulating to 2.4 Gy, or received radiation on days 0, and 14 cumulating to 1.6 Gy. They were then sacrificed on day 21 and day 28. The total number of animals for this group was 16 for the 1.6 and 2.4 Gy groups.

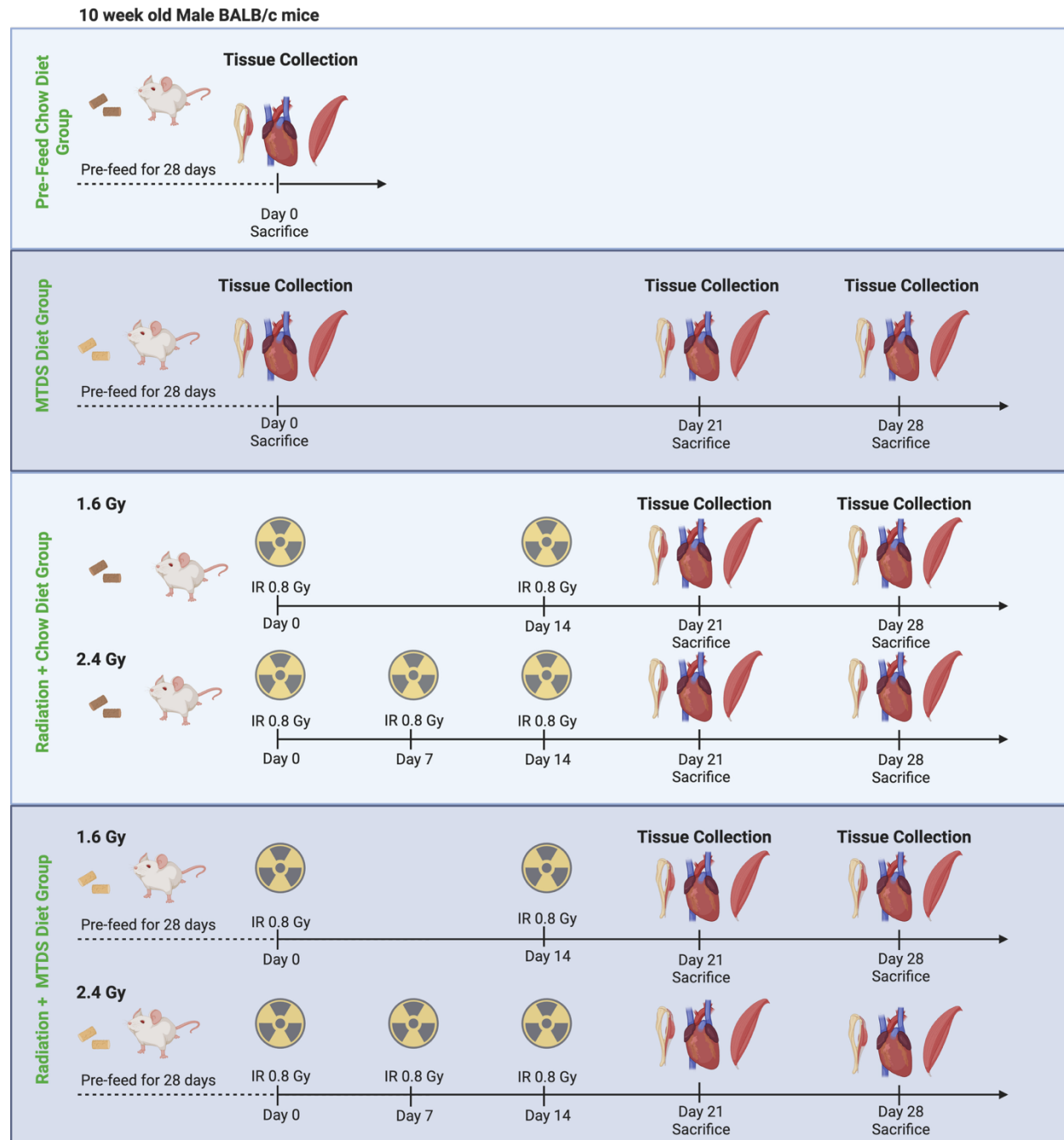


Figure 2. Visual representation of the experimental timeline.

Tissue Collection

At designated study endpoints (day 0, day 21 and day 28) animals were euthanized by cervical dislocation. Body weights were recorded to provide an overall context of systemic health and to contextualize muscle specific changes. Hindlimb muscles, including the tibialis anterior (TA), gastrocnemius and plantaris (GP), quadriceps, and soleus were collected. Tissue from the left leg was collected, weighted and then mounted in Tissue Plus Optimal Cutting Temperature compound (OCT; Fisher Healthcare) and flash frozen liquid nitrogen-cooled isopentane and stored in -80°C for histological analysis. Tissue harvested from the right leg were flash frozen in liquid nitrogen and stored in -80°C for biochemical analysis. The heart, liver, eyes, tibia, fibula, and femur were also collected for future assessments.

Analyses

Histological Analysis

Frozen TA, GP and soleus muscles samples mounted in OCT were cut into 10µm cross sections with a cryostat (Thermo Fisher Scientific; Kalamazoo, MI, United States) and placed on Fisherbrand Superforst Plus Slides (Thermo Fisher Scientific) stored in -20°C. All samples were imaged using Nikon Eclipse Ti microscope and analyzed on the NIS- Elements ND2 software (Nikon, Mississauga, ON). Hematoxylin and eosin (H&E) staining was completed using an existing protocol published by Hughes et al⁷¹. Once the cross sections of tissue were imaged, cross sectional area and min Feret data was collected by choosing to circle a total of 150 muscle fibers in four sites in a tissue sample. Centrally-located nuclei in muscle fibers were quantified by counting the number of centrally-located nuclei relative to the total surface area.

F4/80 Macrophage Stain

Tissue mounted in OCT were sectioned into 6µm cross sections and air-dried prior staining. Sections were fixed with 4% paraformaldehyde (PFA) (158127, Sigma-Aldrich) solution at 4°C for 5 minutes. Next, sections were washed with phosphate-buffered saline (PBS) for 5 mins to remove excess fixative. To minimize non-specific binding, sections were blocked using 10% normal goat serum (NGS) (G9023, Sigma-Aldrich) at room temperature for 40 minutes. The primary antibody for macrophages, rat anti-mouse F4/80 (ab16911, Abcam) a marker for murine macrophages, was diluted at 1:100 in PBS and applied to the sections. Slides were then incubated overnight at 4°C, following incubation the sections were washed with PBS. The secondary antibody for macrophages, Alexa Fluor 594 goat anti-rat (A11072, Invitrogen) was diluted at 1:250 and applied for 45 minutes at room temperature. Afterward, sections were washed thoroughly with PBS. Next, slides were blocked with 10% NGS for 30 minutes. The primary antibody, dystrophin anti-rabbit (ab15277, Abcam) was diluted at 1:250, and slides were incubated for 1 hr at room temperature. Following incubation, slides were washed again with PBS. The secondary antibody for dystrophin, Alexa Fluor 488 goat anti-rabbit (A-11008, Fisher Healthcare), diluted at 1:250, was applied for 45 minutes at room temperature, followed by washing with PBS. Fluoromount with DAPI (4,6-diamidino-2-phenylindole) (501128966, Invitrogen) was applied to slides and cover slipped. Slides were imaged the next day with using Nikon Eclipse Ti microscope and analyzed on the NIS- Elements ND2 software (Nikon, Mississauga, ON). F4/80 macrophage marker was visualized as red fluorescence overlapping with DAPI in blue. Dystrophin was visualised as green fluorescence and DAPI stain muscle and macrophage nuclei in blue fluorescence. Analysis of the stain include counting the number of

macrophages within a muscle fiber (referred herein as intrafiber macrophages) divided by the total number of macrophages present in the tissue and expressed as a percentage.

Statistical Analysis

All data underwent the Grubbs outlier test to remove any outliers in the data. This test was selected because it is specifically designed to detect a single outlier in a dataset, this minimizes the risk of overcorrecting or removing valid data points. Following removing of outliers, a one-way ANOVA with preplanned comparisons was performed to compare differences across groups at the two time points using GraphPad Prism Version 10.5.0 software (GraphPad, San Diego, CA, USA). Preplanned comparisons consisted of control versus the MTDS control, control versus Radiation (Rad) + control diet, the MTDS diet versus Rad + MTDS diet, and Rad + control diet versus Rad + MTDS diet. Significance was accepted at $p < 0.05$ and data was expressed as mean \pm SEM.

RESULTS

Body Weights

Body weights were recorded for all animals in each group at day 21 and day 28. There were no differences in body weights between the MTDS diet control and control diet groups, at either timepoint (Fig. 3). In the groups exposed to 1.6 Gy there were no differences between treatments at both day 21 and day 28 (Fig. 3A, B). In the 2.4 Gy dosage group, at day 21 the Rad 2.4 Gy group + control diet had significantly lower body weights compared to both the control and Rad 2.4 Gy + MTDS diet group (Fig. 3C). However, at day 28, these differences were no longer present.

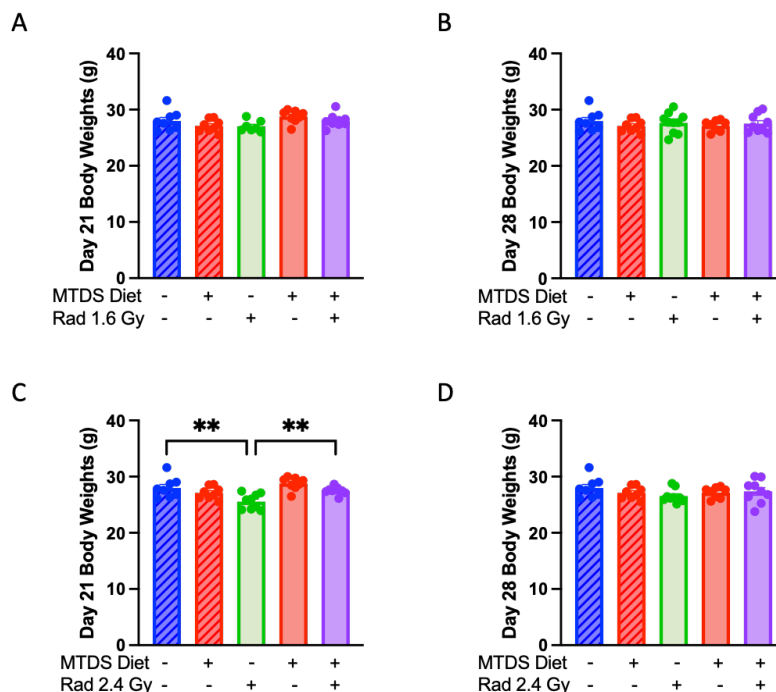


Figure 3. Changes in body weights at day 21 and day 28 following exposure to 1.6 or 2.4 Gy of IR. (A) Day 21 body weights at 1.6 Gy. (B) Day 28 body weights at 1.6 Gy. (C) Day 21 body weights at 2.4 Gy. (D) Day 28 body weights at 2.4Gy. Experimental groups were organized by dietary treatment and radiation dose indicated by pluses and minuses. The striped blue bar represents the control group harvested at day 0, these mice were only on the control diet, n=8. The striped red bar represents the MTDS control harvested at day 0, these mice were only on the MTDS diet, n=8. The green bar represents mice who received the control diet and were exposed to radiation (Rad + control diet), n=9. The solid red bar represents mice who were on the MTDS diet harvested either on day 21 or day 28 and not exposed to radiation, n=8. The purple bar represents mice who were on the MTDS diet and exposed to radiation (Rad + MTDS diet), n=9. Bars represent mean \pm standard error of the mean. A one-way ANOVA was performed, with the Sidak's multiple comparisons test between the following pre-planned comparisons: control vs. MTDS control, control vs. Rad 2.4 Gy + control diet, MTDS diet vs. Rad + MTDS diet, and Rad + control diet vs. Rad + MTDS diet. Asterisks denote statistical significance (* $p < 0.05$, ** $p < 0.01$, *** $p < 0.001$, **** $p < 0.0001$).

Skeletal Muscle Mass.

Tibialis anterior (TA), quadriceps, gastrocnemius and plantaris (GP), and soleus muscles were collected and weighed at day 21 and day 28 and their weights were recorded. All muscle weights were normalized to body weights and reported as a percentage.

At day 21 the Rad 1.6 Gy + control diet had significantly lower muscle/body weight ratios in the TA compared to control (Fig. 4A) and this difference was visible at day 28 as well (Fig. 4B). At both day 21 and day 28, there were no differences in the TA muscle/body weight ratios in the Rad 1.6 Gy + MTDS diet compared to the MTDS diet alone. In the 2.4 Gy group at day 21, the control group had significantly higher TA muscle/body weight ratios compared to the MTDS control group (Fig. 4C). At day 28, the difference between the control and the MTDS control was still visible, and interestingly the Rad 2.4 Gy + MTDS group had significantly lower TA muscle/body weight ratios as compared to the Rad 2.4 Gy + control diet and the MTDS diet groups (Fig. 4D).

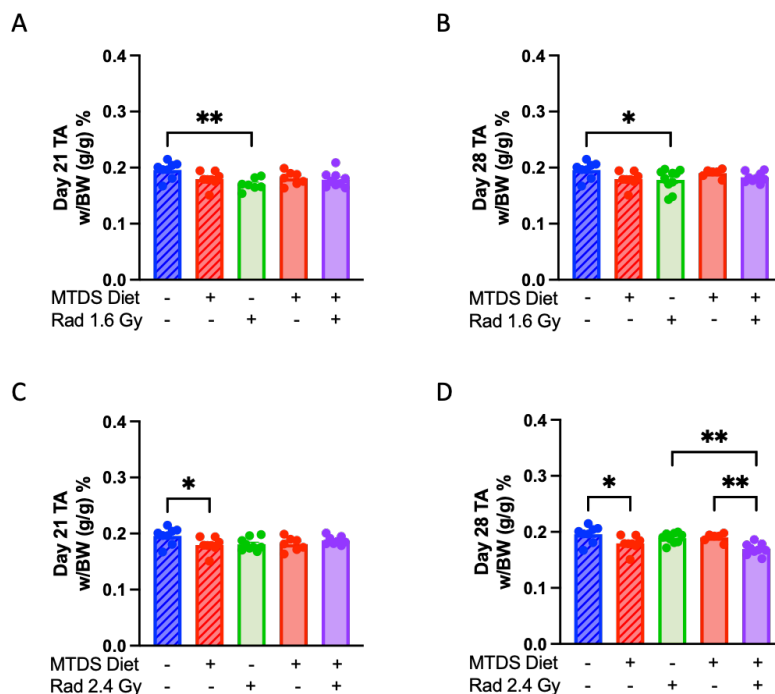


Figure 4. Tibialis anterior (TA) muscle/body weight ratios (%) at day 21 and day 28

following exposure to 1.6 or 2.4 Gy of IR. (A) Day 21 TA muscle/body weight ratios at 1.6 Gy. (B) Day 28 TA muscle/body weight ratios at 1.6 Gy. (C) Day 21 TA muscle/body weight ratios at 2.4 Gy. (D) Day 28 TA muscle/body weight ratios at 2.4Gy. Experimental groups were organized by dietary treatment and radiation dose indicated by pluses and minuses. The striped blue bar represents the control group harvested at day 0, these mice were only on the control diet, n=8. The striped red bar represents the MTDS control harvested at day 0, these mice were only on the MTDS diet, n=8. The green bar represents mice who received the control diet and were exposed to radiation (Rad + control diet), n=9. The solid red bar represents mice who were on the MTDS diet harvested either on day 21 or day 28 and not exposed to radiation, n=8. The purple bar represents mice who were on the MTDS diet and exposed to radiation (Rad + MTDS diet), n=9. Bars represent mean \pm standard error of the mean. A one-way ANOVA was performed, with the Sidak's multiple comparisons test between the following pre-planned comparisons: control vs. MTDS control, control vs. Rad 2.4 Gy + control diet, MTDS diet vs. Rad + MTDS diet, and Rad + control diet vs. Rad + MTDS diet. Asterisks denote statistical significance (* $p < 0.05$, ** $p < 0.01$, *** $p < 0.001$, **** $p < 0.0001$).

Quadricep muscle/body weight ratios remained consistent across all groups at 1.6 Gy on day 21. At day 28, the Rad 1.6 Gy + MTDS group had a significant decrease in the quadricep muscle/body weight ratios weights compared to the MTDS group. However, no differences were seen between the Rad 1.6 Gy + control diet and the Rad 1.6 + MTDS groups (Fig. 5B). At the 2.4 Gy exposure, there were no differences between quadricep muscle/body weight ratios across all treatment groups.

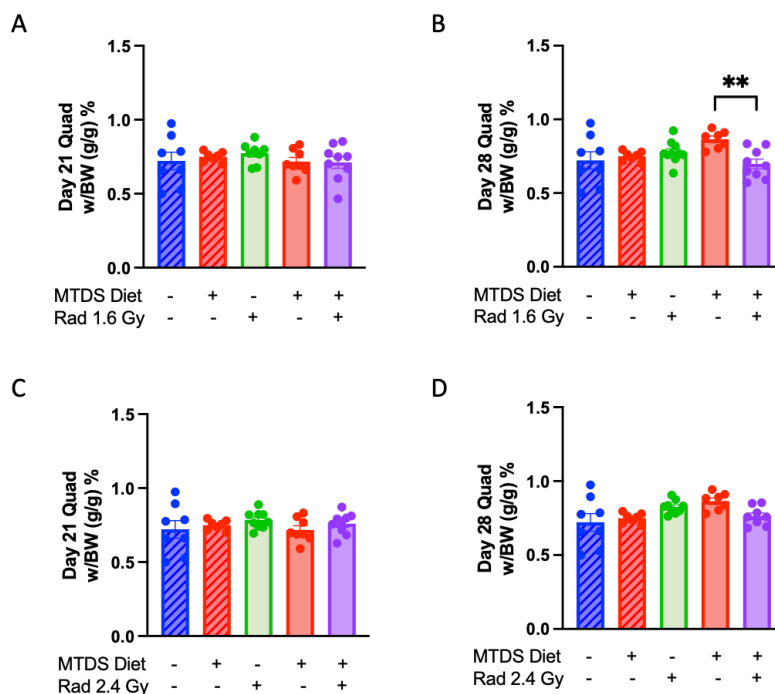


Figure 5. Quadriceps muscle/body weight ratios (%) at day 21 and day 28 following exposure to 1.6 or 2.4 Gy of IR. (A) Day 21 quadriceps muscle/body weight ratios at 1.6 Gy. (B) Day 28 quadriceps muscle/body weight ratios at 1.6 Gy. (C) Day 21 quadriceps muscle/body weight ratios at 2.4 Gy. (D) Day 28 quadriceps muscle/body weight ratios at 2.4Gy. Experimental groups were organized by dietary treatment and radiation dose indicated by pluses and minuses. The striped blue bar represents the control group harvested at day 0, these mice were only on the control diet, n=8. The striped red bar represents the MTDS control harvested at day 0, these mice were only on the MTDS diet, n=8. The green bar represents mice who received the control diet and were exposed to radiation (Rad + control diet), n=9. The solid red bar represents mice who were on the MTDS diet harvested either on day 21 or day 28 and not exposed to radiation, n=8. The purple bar represents mice who were on the MTDS diet and exposed to radiation (Rad + MTDS diet), n=9. Bars represent mean \pm standard error of the mean. A one-way ANOVA was performed, with the Sidak's multiple comparisons test between the following pre-planned comparisons: control vs. MTDS control, control vs. Rad 2.4 Gy + control diet, MTDS diet vs. Rad + MTDS diet, and Rad + control diet vs. Rad + MTDS diet. Asterisks denote statistical significance (* $p < 0.05$, ** $p < 0.01$, *** $p < 0.001$, **** $p < 0.0001$).

Muscle/body weight ratios in the GP remained consistent in the 1.6 Gy exposure group on day 21. However, on day 28, the Rad 1.6 Gy + control diet had significantly higher GP muscle/body weight ratios compared to the Rad 1.6Gy + MTDS diet (Fig. 6B). In the 2.4 Gy cohort at day 21, the Rad 2.4 + MTDS group had significantly higher GP muscle/body weight ratios compared to both Rad 2.4 Gy + control diet and the MTDS diet groups (Fig. 6C). However, at day 28 no differences were seen between treatment groups.

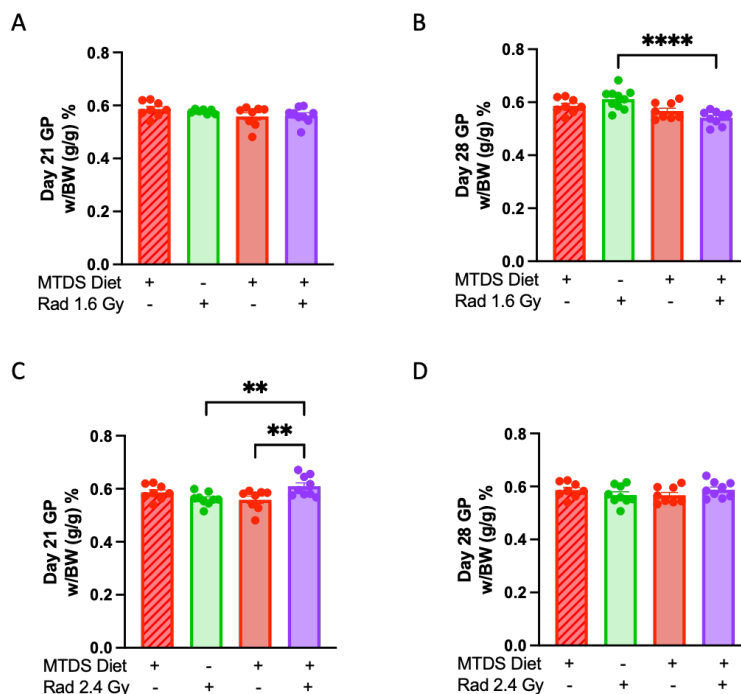


Figure 6. Gastrocnemius and plantaris (GP) muscle/body weight ratios (%) at day 21 and day 28 following exposure to 1.6 or 2.4 Gy of IR. (A) Day 21 GP muscle/body weight ratios at 1.6 Gy. (B) Day 28 GP muscle/body weight ratios at 1.6 Gy. (C) Day 21 GP muscle/body weight ratios at 2.4 Gy. (D) Day 28 GP muscle/body weight ratios at 2.4Gy. Experimental groups were organized by dietary treatment and radiation dose indicated by pluses and minuses. The striped red bar represents the MTDS control harvested at day 0, these mice were only on the MTDS diet, n=8. The green bar represents mice who received the control diet and were exposed to radiation (Rad + control diet), n=9. The solid red bar represents mice who were on the MTDS diet harvested either on day 21 or day 28 and not exposed to radiation, n=8. The purple bar represents mice who were on the MTDS diet and exposed to radiation (Rad + MTDS diet), n=9. Bars represent mean \pm standard error of the mean. A one-way ANOVA was performed, with the Sidak's multiple comparisons test between the following pre-planned comparisons: MTDS diet vs. Rad + MTDS diet, and Rad + control diet vs. Rad + MTDS diet. Asterisks denote statistical significance (* p<0.05, ** p<0.01, *** p<0.001, **** p<0.0001).

There were no differences in soleus muscle/body weight ratios on both day 21 and day 28 (Fig. 7A, B) in the 1.6 Gy cohort. Interestingly, on day 21 (Fig. 7A) the Rad 1.6 Gy + control diet group exhibited slightly higher soleus muscle/body weight ratios compared to the MTDS diet ($p = 0.1078$) although not significant. On day 28 there were no differences in soleus muscle/body weight ratios (Fig. 7B). In the 2.4 Gy cohort there were no differences in soleus muscle/body weight ratios across all time points in each experimental group.

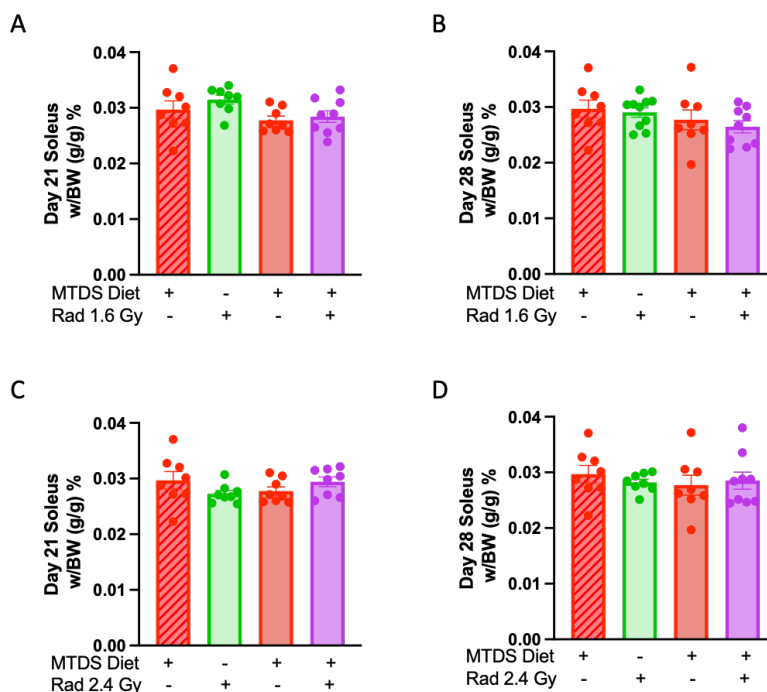


Figure 7. Soleus muscle/body weight ratios (%) at day 21 and day 28 following exposure to 1.6 or 2.4 Gy of IR. (A) Day 21 soleus muscle/body weight ratios at 1.6 Gy. (B) Day 28 soleus muscle/body weight ratios at 1.6 Gy. (C) Day 21 soleus muscle/body weight ratios at 2.4 Gy. (D) Day 28 soleus muscle/body weight ratios at 2.4 Gy. Experimental groups were organized by dietary treatment and radiation dose indicated by pluses and minuses. The striped red bar represents the MTDS control harvested at day 0, these mice were only on the MTDS diet, n=8. The green bar represents mice who received the control diet and were exposed to radiation (Rad + control diet), n=9. The solid red bar represents mice who were on the MTDS diet harvested either on day 21 or day 28 and not exposed to radiation, n=8. The purple bar represents mice who were on the MTDS diet and exposed to radiation (Rad + MTDS diet), n=9. Bars represent mean \pm standard error of the mean. A one-way ANOVA was performed, with the Sidak's multiple comparisons test between the following pre-planned comparisons: MTDS diet vs. Rad + MTDS diet, and Rad + control diet vs. Rad + MTDS diet. Asterisks denote statistical significance (* $p < 0.05$, ** $p < 0.01$, *** $p < 0.001$, **** $p < 0.0001$).

Cross-Sectional Area and Min Feret Values of the TA.

To further characterize the changes in muscle weights, cross sectional area and min Feret of H&E-stained TA muscles were analyzed. In the 1.6 Gy cohort at day 21, it was observed that Rad 1.6 Gy + control diet group had significantly larger cross-sectional area, but not min Feret compared to control (Fig. 8A, E). Furthermore Rad 1.6 Gy + MTDS diet had significantly lower cross-sectional area and min Feret compared to the MTDS diet (Fig. 8A, E). At day 28, Rad 1.6 Gy + control diet had a significantly higher cross-sectional area and min Feret values compared to control and Rad 1.6 Gy + MTDS diet (Fig. 8B, F). Interestingly, min Feret values of Rad 1.6 Gy + MTDS diet group were lower compared to MTDS diet at day 21 (Fig.8F).

At day 21 in the 2.4 Gy cohort, Rad 2.4 Gy + control diet had a significantly larger cross-sectional area, but not min Feret, compared to control (Fig. 8C, G). Rad 2.4 Gy + MTDS had larger min Feret values compared to the MTDS diet (Fig. 8G). At day 28, both cross-sectional area and min Feret values for the Rad 2.4 Gy + control diet group were significantly larger compared to control (Fig. 8D, H). At both radiation doses, groups exposed to radiation on the MTDS diet trended towards smaller cross-sectional area and min ferrets, compared to animals exposed to radiation on the normal diet.

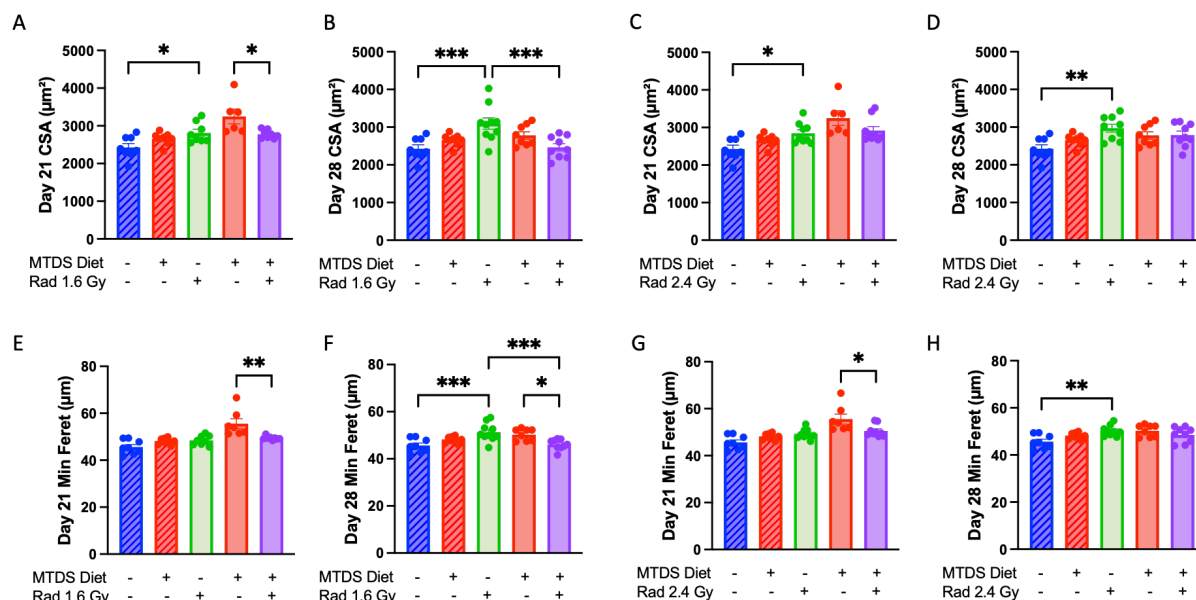


Figure 8. TA cross-sectional area and min Feret diameter at day 21 and day 28 following exposure to 1.6 or 2.4 Gy of IR. (A) Day 21 cross sectional area at 1.6 Gy. (B) Day 28 cross sectional area at 1.6 Gy. (C) Day 21 cross sectional area at 2.4 Gy. (D) Day 28 cross sectional area at 2.4 Gy. (E) Day 21 min Feret at 1.6 Gy. (F) Day 28 min Feret at 1.6 Gy. (G) Day 21 min Feret at 2.4 Gy. (H) Day 28 min Feret at 2.4Gy. Cross-sectional area (in μm^2) and min Feret (μm) was recorded at different time points across experimental groups using NIS elements software. Experimental groups were organized by dietary treatment and radiation dose indicated by pluses and minuses. The striped blue bar represents the control group harvested at day 0, these mice were only on the control diet, n=8. The striped red bar represents the MTDS control harvested at day 0, these mice were only on the MTDS diet, n=8. The green bar represents mice who received the control diet and were exposed to radiation (Rad + control diet), n=9. The solid red bar represents mice who were on the MTDS diet harvested either on day 21 or day 28 and not exposed to radiation, n=8. The purple bar represents mice who were on the MTDS diet and exposed to radiation (Rad + MTDS diet), n=9. Bars represent mean \pm standard error of the mean. A one-way ANOVA was performed, with the Sidak's multiple comparisons test between the following pre-planned comparisons: control vs. MTDS control, control vs. Rad 2.4 Gy + control diet, MTDS diet vs. Rad + MTDS diet, and Rad + control diet vs. Rad + MTDS diet. Asterisks denote statistical significance (* $p<0.05$, ** $p<0.01$, *** $p<0.001$, **** $p<0.0001$).

Quantification of Centrally-located Nuclei

To further characterize the impact of radiation on skeletal muscle the number of centrally-located nuclei relative to surface area was quantified in the TA and GP muscles. Centrally-located nuclei in muscle fibers can originate from either activated satellite cells which fuse to aid in muscle regeneration and repair, or macrophages that infiltrate damaged fibers to facilitate tissue remodelling and phagocytosis.

In the 1.6 Gy cohort at both day 21 and day 28, there was an increase in centrally-located nuclei in the MTDS control group compared to control. It was also observed that there was a significant increase in centrally-located nuclei in the Rad 1.6 Gy + control diet compared to control (Fig. 9B, C). Although not significant Rad 1.6 Gy + control diet trends towards higher number of centrally-located nuclei compared to the Rad 1.6 Gy + MTDS diet ($p=0.0641$) at day 21 (Fig. 9B).

At day 21 in the 2.4 Gy cohort, there was a significant increase in centrally-located nuclei in the Rad 2.4 Gy + control diet group compared to the control and the Rad 2.4 Gy + MTDS diet groups (Fig. 9D). At day 28, there was still a significant increase in centrally-located nuclei in the Rad 2.4 Gy + control diet group compared to the control group, however there were no longer differences between the Rad 2.4 Gy + control diet and the Rad 2.4 Gy + MTDS diet groups (Fig. 9E). At both timepoints, the Rad 2.4 Gy + MTDS diet had a significantly larger numbers of centrally-located nuclei compared to the MTDS diet (Fig. 9D).

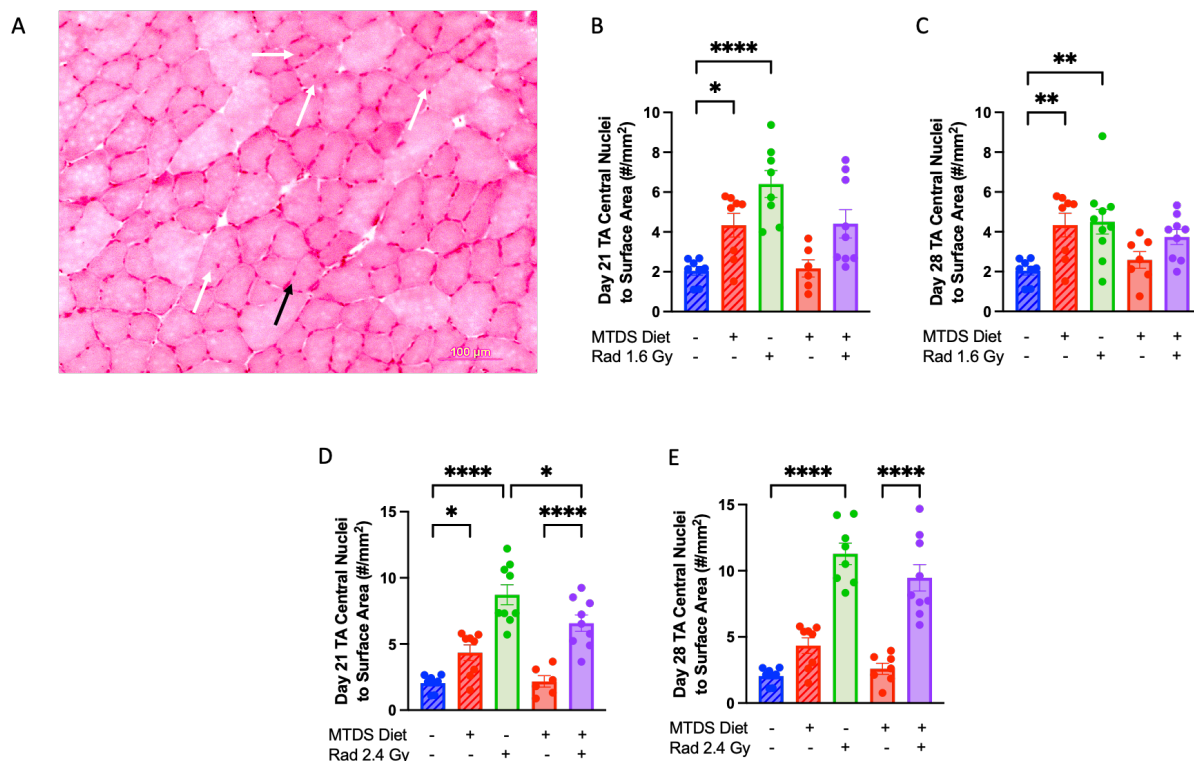


Figure 9. Number of centrally-located nuclei relative to surface area in the TA muscle at day 21 and day 28 following exposure to 1.6 or 2.4 Gy of IR. (A) Representative image of centrally-located nuclei in a TA muscle cross section from the Rad 1.6 Gy + control diet, day 21 group. White arrows point to centrally-located nuclei, and the black arrow points to peripheral nuclei. Muscle cross sections embedded in OCT underwent H&E staining. (B) Day 21 number of centrally-located nuclei relative to surface area in the TA at 1.6 Gy. (C) Day 28 number of centrally-located nuclei relative to surface area in the TA at 1.6 Gy. (D) Day 21 number of centrally-located nuclei relative to surface area in the TA at 2.4 Gy. (E) Day 28 number of centrally-located nuclei relative to surface area in the TA at 2.4 Gy. Experimental groups were organized by dietary treatment and radiation dose indicated by pluses and minuses. The striped blue bar represents the control group harvested at day 0, these mice were only on the control diet, n=8. The striped red bar represents the MTDS control harvested at day 0, these mice were only on the MTDS diet, n=8. The green bar represents mice who received the control diet and were exposed to radiation (Rad + control diet), n=9. The solid red bar represents mice who were on the MTDS diet harvested either on day 21 or day 28 and not exposed to radiation, n=8. The purple bar represents mice who were on the MTDS diet and exposed to radiation (Rad + MTDS diet), n=9. Bars represent mean \pm standard error of the mean. A one-way ANOVA was performed, with the Sidak's multiple comparisons test between the following pre-planned comparisons: control vs. MTDS control, control vs. Rad 2.4 Gy + control diet, MTDS diet vs. Rad + MTDS diet, and Rad + control diet vs. Rad + MTDS diet. Asterisks denote statistical significance (* $p < 0.05$, ** $p < 0.01$, *** $p < 0.001$, **** $p < 0.0001$).

GP muscles were also analyzed for changes in centrally-located nuclei to surface area numbers and displayed similar trends to that of the TA muscles. The Rad 1.6 Gy + control diet group exhibited significantly higher numbers of centrally-located nuclei compared to the control and the Rad 1.6 Gy + MTDS diet group at day 21 (Fig. 10A). Interestingly, the Rad 1.6 Gy + MTDS diet group had significantly lower numbers of centrally-located nuclei compared to the MTDS diet group at day 21 (Fig. 10A), however this difference disappeared on day 28 (Fig. 10B). On day 28, the Rad 1.6 Gy + control diet group continued to express higher numbers of centrally-located nuclei compared to the control group.

In the 2.4 Gy cohort on day 21 and day 28 the Rad 1.6 Gy + control diet group exhibited significantly higher numbers of centrally-located nuclei compared to the control group (Fig. 10C, D). On day 28, the Rad 2.4 Gy + control diet group had significantly larger number of centrally-located nuclei compared to the Rad 2.4 Gy + MTDS diet group (Fig. 10D). No differences between the MTDS diet and the Rad 2.4 Gy + MTDS groups were seen at both timepoints.

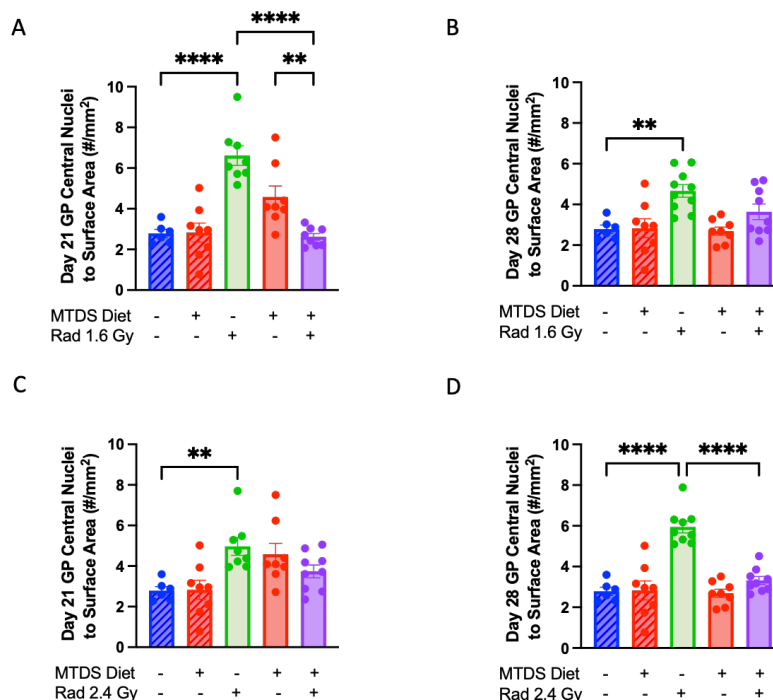


Figure 10. Number of centrally-located nuclei relative to surface area in the GP muscle at day 21 and day 28 following exposure to 1.6 or 2.4 Gy of IR. (A) Day 21 number of centrally-located nuclei relative to surface area in the GP at 1.6 Gy. (B) Day 28 number of centrally-located nuclei relative to surface area in the GP at 1.6 Gy. (C) Day 21 number of centrally-located nuclei relative to surface area in the GP at 2.4 Gy. (D) Day 28 number of centrally-located nuclei relative to surface area in the GP at 2.4 Gy. Experimental groups were organized by dietary treatment and radiation dose indicated by pluses and minuses. The striped blue bar represents the control group harvested at day 0, these mice were only on the control diet, n=8. The striped red bar represents the MTDS control harvested at day 0, these mice were only on the MTDS diet, n=8. The green bar represents mice who received the control diet and were exposed to radiation (Rad + control diet), n=9. The solid red bar represents mice who were on the MTDS diet harvested either on day 21 or day 28 and not exposed to radiation, n=8. The purple bar represents mice who were on the MTDS diet and exposed to radiation (Rad + MTDS diet), n=9. Bars represent mean \pm standard error of the mean. A one-way ANOVA was performed, with the Sidak's multiple comparisons test between the following pre-planned comparisons: control vs. MTDS control, control vs. Rad 2.4 Gy + control diet, MTDS diet vs. Rad + MTDS diet, and Rad + control diet vs. Rad + MTDS diet. Asterisks denote statistical significance (* $p < 0.05$, ** $p < 0.01$, *** $p < 0.001$, **** $p < 0.0001$).

Intrafiber Macrophage Quantification

Macrophages within muscle fibers are indicative of muscle fibers that are damaged and undergoing phagocytosis. Macrophages inside muscle fibers (referred to as intrafiber macrophages) were counted using an f4/80 stain and divided by the total number of macrophages within the image. On both day 21 and day 28, there was a significant increase in the percentage of intrafiber macrophages in the Rad 1.6 Gy + control diet group compared to the control and the Rad 1.6 Gy + MTDS diet groups. Additionally, at both timepoints no differences were seen between the Rad 1.6 Gy + MTDS and the MTDS diet groups.

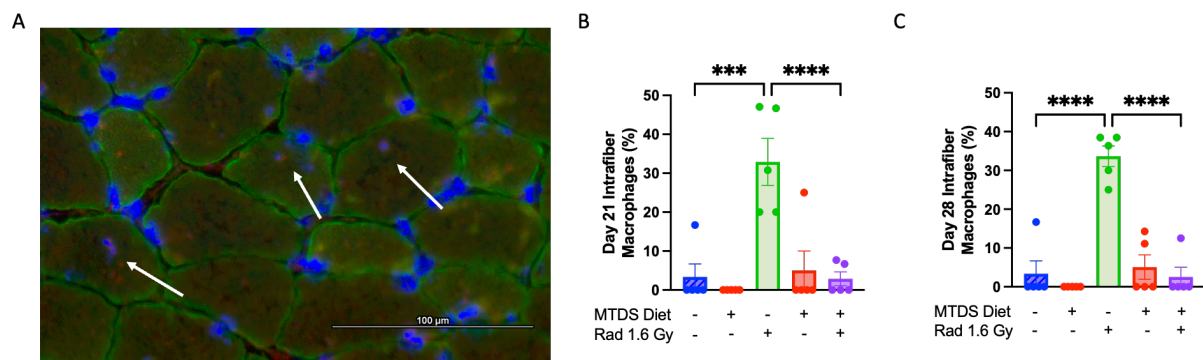


Figure 11. Percentage of intrafiber macrophages in the TA muscle at day 21 and day 28 following exposure to 1.6 or 2.4 Gy of IR. (A) Representative image of F4/80 Macrophage stain in a TA cross section from the Rad 1.6 Gy + control diet, day 28 group. A macrophage within the muscle fiber (intrafiber) is stained (red), with DAPI (blue) and dystrophin staining the muscle sarcolemma (green). The arrows point to macrophages within a muscle fiber. (B) Percentage of intrafiber macrophages in the 1.6 Gy group on Day 21. (C) Percentage of intrafiber macrophages in the 1.6 Gy group on Day 28. Experimental groups were organized by dietary treatment and radiation dose indicated by pluses and minuses. The striped blue bar represents the control group harvested at day 0, these mice were only on the control diet, n=5. The striped red bar represents the MTDS control harvested at day 0, these mice were only on the MTDS diet, n=5. The green bar represents mice who received the control diet and were exposed to radiation (Rad + control diet), n=5. The solid red bar represents mice who were on the MTDS diet harvested either on day 21 or day 28 and not exposed to radiation, n=5. The purple bar represents mice who were on the MTDS diet and exposed to radiation (Rad + MTDS diet), n=5. Bars represent mean \pm standard error of the mean. A one-way ANOVA was performed, with the Sidak's multiple comparisons test between the following pre-planned comparisons: control vs. MTDS control, control vs. Rad 2.4 Gy + control diet, MTDS diet vs. Rad + MTDS diet, and Rad + control diet vs. Rad + MTDS diet. Asterisks denote statistical significance (* $p < 0.05$, ** $p < 0.01$, *** $p < 0.001$, **** $p < 0.0001$).

DISCUSSION

Ionizing radiation (IR) exposure is one of the most pressing challenges during space travel as it has detrimental effects on skeletal muscle tissue, leading to various forms of damage and impairment. The impact of radiation on muscles involves a cascade of events including inflammation^{45,46}, oxidative stress^{72,73}, and direct damage to muscle cells with the inhibition of satellite cells^{46,51} ultimately resulting in compromised muscle function and structure. The current body of literature related to radiation exposure and skeletal muscle outcomes has focused predominantly on higher doses of IR exposure which is relevant to cancer therapy and subsequently its effects on skeletal muscle. However, there is a considerable gap in the research regarding the effects of lower doses of IR exposure such as those relevant to spaceflight. Furthermore, current countermeasures of exercise and shielding are not wholly protective against IR exposure, and this underscores the potential risks of inadequate protection during long term space mission such as those to Mars^{74–76}. This current study sheds some light on the effects of spaceflight relevant doses of IR on the skeletal muscles, as well the potential effectiveness of the Multi-Targeted Dietary Supplement (MTDS) in mitigating the negative impacts of radiation exposure. This study demonstrated that the MTDS preserved body weights post-radiation exposure and maintained lower CSA and min Feret values compared to the control diet, suggesting protection against radiation-induced muscle edema. Additionally, it provided cellular level protection by decreasing the number of centrally-located nuclei and macrophages, markers of muscle damage and inflammation, respectively.

In the present study, 1.6 and 2.4 Gy were chosen for the level of radiation exposure as these are more relevant to those that may be experienced by astronauts. In addition, the selection of two distinctly different radiation doses allowed an investigation of the potential effective

threshold of the MTDS. The lowest limit of radiation exposure (1.6 Gy) was chosen because exposure to less than 1 Gy, especially 0.4–0.5 Gy was demonstrated to be protective^{77,78} and as a result a higher dosage of radiation was chosen in order promote cellular damage. Furthermore, a slightly higher dose, than the lifetime limit of 1 Gy, was chosen as mice are more radiation tolerant compared to humans⁷⁹. On the other hand, the 2.4 Gy dose was chosen to be reflective of longer duration space flight missions, such as those to mars which can last up to 2 years⁸⁰. The duration of the mission can increase the degree at which astronauts are exposed to radiation^{74,80} and thus this dosage serves as a higher dosage, which is known to have negative impacts on the human body^{81–83}, to test the effectiveness of the MTDS in mitigating any damage.

In order to determine the effects that the two doses of IR had on overall body composition, body weight was measured. It was observed that exposure to 1.6 Gy radiation did not negatively impact overall body weight regardless of the group or time point. At the higher dose, 2.4 Gy, a change in body weight was observed in the irradiated group at day 21. However, mice on the MTDS diet did not show any significant alterations. This suggests that the MTDS diet may help protect against radiation induced weight loss at the higher dose. However, body weights were observed to have recovered by at day 28. The doses of IR chosen may not be large enough to have significant changes on body weights. This is further supported as existing literature had shown that exposure to IR results in a reduction in body weights, however these studies exposed mice to larger doses of radiation^{84,85}, such as 16 Gy⁵⁴, which is relevant to cancer therapy. The findings of this study are aligned with existing studies where weight loss in space is driven primarily by microgravity^{21,86,87} and not radiation exposure. Future studies investigating the dual

impacts of IR and microgravity would provide insight into how both stresses affect astronauts in space.

Changes in body weights can be influenced by various factors such as loss of adipose tissue, recent food intake, and hydration status. Therefore, to better understand tissue level changes in muscle, the excised hindlimb muscles were normalized to body weight. Muscle weights were normalized to body weights to account for individual variations in overall body sizes, to provide a more accurate comparison between groups. In the present study it was determined that following exposure to both radiation doses the TA, quadricep and GP in the control diet group showed higher muscle/body weight ratios as compared to those on the MTDS diet. This was an interesting finding, as it seems contrary what one would expect given that radiation had previously been shown to induce muscle damage^{45,46,51,54–56,88}. To further understand these changes, the CSA and min Feret values were measured in the TA muscle group, and it was determined that groups exposed to IR on the control diet compared to those on the MTDS diet had increased CSA and min Feret diameters at both timepoints at both IR doses. Furthermore, at the higher dose of 2.4 Gy there were no differences in CSA and min Feret between control and the MTDS diets. However, at 1.6 Gy on day 28 the MTDS diet group had lower CSA and min Feret values compared to the control diet group post exposure to IR. This provides further evidence of a dose dependent response on muscle damage, with the MTDS offering protective effects at 1.6 Gy at the later timepoint indicating the long-term benefits. Taken together these findings suggest that post radiation edema and not hypertrophy, is the underlying reason for the observed increased muscle mass. While very few studies have examined muscle swelling post IR exposure, it is hypothesised that the IR damage to endothelial cells increases vascular

permeability resulting in edema in tissues^{20,89}. Furthermore, studies have shown that whole body exposure to IR, although at larger doses, cause fluid retention and swelling^{20,89,90}.

Interestingly, soleus muscle did not demonstrate any significant differences in the muscle/body weight ratio following IR exposure. The soleus muscle is primarily composed of Type I, slow twitch fibers, and some Type IIA fibers and therefore may be resistant to IR induced skeletal muscle damage⁹¹. Previous literature suggests that due to the soleus being composed of primarily muscle fibers expressing a high degree of SDH activity (Type I), an indirect measure of mitochondrial content, allows it to maintain constant fiber size even after exposure to IR⁵⁴. This suggests that Type I fibers may be more resistant to IR induced damage due to their high mitochondrial content being able to combat radiation induced oxidative stress⁹². Additional studies have noted that IR exposure results in smaller Type IIA and IIB fibers^{54,93}, suggesting muscle fiber specific changes. This knowledge provides evidence to support the notion of muscle specific changes as the TA, quadriceps and GP are more IR sensitive due to mainly being composed of Type IIA and IIB fibers. It is very interesting to note that both Type I and Type IIA fibers are mitochondrial dense, and it is known mitochondria are a very high source of reactive oxygen species^{82,83}, it would be expected after IR exposure these fiber types would actually be reduced. However, our findings suggest the opposite effect, which suggest the prevalence of Type I fibers maybe due to the baseline antioxidant capacity of mitochondria rich fibers. To support this idea, studies have demonstrated that post muscle damage mitochondria rich fibers are able to maintain reliance due to their antioxidant enzymes such as superoxide dismutase, catalase and glutathione peroxidase, however these studies have mainly been focused on exercise mediated skeletal muscle damage^{94–96}. These papers demonstrate mitochondrial response to

skeletal muscle injury is complex and additional research needs to be completed to understand the effects of IR on mitochondrial changes in muscle fiber types.

To further assess the extent of muscle damage post IR exposure, muscle tissue cross sections from the TA were quantified for centrally-located nuclei, a marker of muscle regeneration after injury. Centrally-located nuclei can either be satellite cells donating their nuclei to help repair the muscle fiber or macrophages helping to phagocytose the muscle fiber. In the present study an increase in centrally-located nuclei were observed in the control diet group in both the TA and GP muscles at both radiation doses and timepoints. Exposure to 1.6 Gy seems to have less of a damaging effect compared to the 2.4 Gy in the TA at both timepoints. This is demonstrated by larger numbers of centrally-located nuclei post radiation exposure in the day 21 in the control diet group compared to day 28, suggesting partial recovery in both muscles. In the 2.4 Gy group post radiation exposure, centrally-located nuclei numbers were lower in the control diet group on day 21, and increase on day 28, suggesting more extensive damage to the muscle that is continuing to repair. The MTDS diet consistently demonstrated fewer centrally-located nuclei at all timepoints, providing strong evidence that the MTDS may be effective in mitigating muscle damage. Our findings are in agreement with previous literature which have also shown an increase in centrally-located nuclei following IR exposure at a dose as low as 0.24 Gy^{54,93}. Previous studies commonly used a H&E stain to quantify centrally-located nuclei, however this type of stain does not allow for the determination of what the nuclei could be. Additional cell-specific staining, such as a Pax7 stain to analyze for satellite cells⁵⁹, would provide a more fulsome picture to investigate muscle regeneration following IR exposure.

To provide further characterization of the centrally-located nuclei observed, an F4/80 macrophage stain on TA samples was conducted. Based on previous literature, intrafiber

macrophages are pro-inflammatory M1 macrophages which are responsible for muscle phagocytosis⁹⁷, and therefore these macrophages were chosen to be quantified. It was observed that radiation exposure resulted in a significant increase in intrafiber macrophages compared to the total number of macrophages and the MTDS diet mitigated this effect. Previous studies have shown that an increase in macrophage content was observed immediately after exposure to radiation^{45,98} suggesting an acute effect. The current findings demonstrate that elevated intrafiber macrophage levels persist for up to two weeks following IR exposure, clearly demonstrating that IR exposure results in long-term muscle injury and inflammation. To our knowledge, this is the first study to examine macrophages responses at space flight relevant doses of IR exposure at later timepoints.

In conclusion, this study provides novel insights into the effects of spaceflight relevant exposure of IR on skeletal muscle health and highlights the protective capability of the MTDS as potential intervention. It was demonstrated that at two doses, 1.6 and 2.4 Gy, can induce considerable muscle specific changes, as evidenced by an increase in CSA and min Feret, suggesting post-radiation edema as well as increases in centrally-located nuclei and intrafiber macrophages. The severity of these changes was mitigated by the MTDS, indicating its efficacy in protecting muscle integrity and reducing muscle damage, especially at the lower dose. This makes the MTDS a strong candidate as a potential intervention against IR induced muscle damage. Our findings provide strong evidence in muscle specific radiation sensitivity as suggested by the differences in muscle/body weight ratio in the TA, quadriceps, GP and soleus muscles. Additionally, the time frame used in this current study demonstrates that the long-term impact of IR may be more profound than previously recognized and suggests that skeletal muscle may be more sensitive to IR than previously thought. This research underscores the need for

further studies to investigate the long-term effects of IR exposure on muscle health and also supports the need for further investigations utilizing the MTDS as it appears to be a promising intervention for preserving skeletal muscle health during extended space missions.

FUTURE DIRECTIONS

Our study showed that exposure to IR has negative effects on skeletal muscle through morphological changes such as increase in centrally-located nuclei and macrophage quantification along with CSA and min Feret measurements. Additional research needs to be completed on having functional analysis of muscle health, such as electrical stimulation (stim). This approach elicits a muscle contraction using electrical impulses^{99,100} and would provide additional information on how exposure to IR effects muscle contraction and regulation, as well as any potential benefits of the MTDS. Furthermore, functional measures are important due to their ability to observe both phenotypic and physiological effects.

Additionally, the MTDS has preclinical evidence indicating its antioxidant properties. Oxidative assays, such a total antioxidant assay, should be conducted to investigate how the MTDS effects skeletal muscles at baseline. Potentially another study collecting muscle samples immediately post radiation, focused on observing the effects of the MTDS on reducing IR induced ROS and DNA damage would provide further evidence of regarding the efficacy of the supplement to reduce IR induced damage.

CSA and min Feret of muscle tissue were analysed in this study and provided preliminary evidence of post radiation swelling as well as muscle specific changes to IR. Conducting an immunofluorescence stain staining for different muscle fibers, would be ideal to further characterize any fiber type shifts as well as muscle remodelling. This study is part of a larger study, which involves hindlimb suspension, a known stimulus which results in fiber type shifts. It would be worthwhile to investigate the dual impacts of both hindlimb suspension and IR on muscle fiber type changes.

Lastly, our study was conducted on male mice, investigating sex differences would better model astronaut demographics and increase the relevance of the MTDS as a potential intervention. Previous literature had shown that estrogen in females is protective in maintaining bone^{101,102} and muscle health¹⁰³ and also suggests that females are less susceptible to IR induced damage. Additionally, females exhibit stronger immune responses than males, suggesting a faster response to muscle damage and leading to faster recovery^{104,105}. These physiological differences should be further studied in the context of testing potential interventions like the MTDS. This would aid in determining whether the MTDS is equally protective in females or whether there is a need for changes in the formulation of the supplement.

REFERENCES

1. Allen DL, Bandstra ER, Harrison BC, et al. Effects of spaceflight on murine skeletal muscle gene expression. *J Appl Physiol*. 2009;106(2):582-592. doi:10.1152/jappphysiol.90780.2008
2. Comfort P, McMahon JJ, Jones PA, et al. Effects of Spaceflight on Musculoskeletal Health: A Systematic Review and Meta-analysis, Considerations for Interplanetary Travel. *Sports Medicine*. 2021;51(10):2097-2114. doi:10.1007/s40279-021-01496-9
3. Yatagai F, Honma M, Dohmae N, Ishioka N. Biological effects of space environmental factors: A possible interaction between space radiation and microgravity. *Life Sci Space Res (Amst)*. 2019;20:113-123. doi:10.1016/j.lssr.2018.10.004
4. Lockard ES, Arch M. *From Hostile to Hospitable: Changing Perceptions of the Space Environment.*; 2015.
5. Montesinos CA, Khalid R, Cristea O, et al. Space radiation protection countermeasures in microgravity and planetary exploration. *Life*. 2021;11(8). doi:10.3390/life11080829
6. Arbeille P, Zuj KA, Macias BR, et al. Lower body negative pressure reduces jugular and portal vein volumes and counteracts the elevation of middle cerebral vein velocity during long-duration spaceflight. *J Appl Physiol*. 2021;131(3):1080-1087. doi:10.1152/jappphysiol.00231.2021
7. Arbeille P, Fomina G, Roumy J, Alferova I, Tobal N, Herault S. Adaptation of the left heart, cerebral and femoral arteries, and jugular and femoral veins during short- and long-term head-down tilt and spaceflights. *Eur J Appl Physiol*. 2001;86(2):157-168. doi:10.1007/s004210100473
8. Moosavi D, Wolovsky D, Depompeis A, et al. The Effects of Spaceflight Microgravity on the Musculoskeletal System of Humans and Animals, with an Emphasis on Exercise as a Countermeasure: A Systematic Scoping Review. *Physiol Res*. 2021;70(2):119-151. doi:10.33549/physiolres.934550
9. Fitts RH, Trappe SW, Costill DL, et al. Prolonged space flight-induced alterations in the structure and function of human skeletal muscle fibres. *Journal of Physiology*. 2010;588(18):3567-3592. doi:10.1113/jphysiol.2010.188508
10. Lambertz D, Rot CP, Kaspranski R, Goubel F. *Gagarin Cosmonauts Training Centre.*; 2001. <http://www.jap.org>
11. Frontera WR, Ochala J. Skeletal Muscle: A Brief Review of Structure and Function. *Behav Genet*. 2015;45(2):183-195. doi:10.1007/s00223-014-9915-y
12. Lee PHU, Chung M, Ren Z, Mair DB, Kim DH. Factors mediating spaceflight-induced skeletal muscle atrophy. *Am J Physiol Cell Physiol*. 2022;322(3):C567-C580. doi:10.1152/ajpcell.00203.2021
13. Restier-Verlet J, El-Nachef L, Ferlazzo ML, et al. Radiation on earth or in space: what does it change? *Int J Mol Sci*. 2021;22(7). doi:10.3390/ijms22073739
14. Chancellor JC, Scott GBI, Sutton JP. Space radiation: The number one risk to astronaut health beyond low earth orbit. *Life*. 2014;4(3):491-510. doi:10.3390/life4030491

15. Hu S, Kim MHY, McClellan GE, Cucinotta FA. *MODELING THE ACUTE HEALTH EFFECTS OF ASTRONAUTS FROM EXPOSURE TO LARGE SOLAR PARTICLE EVENTS.*; 2009. <http://journals.lww.com/health-physics>
16. Kennedy AR. Biological effects of space radiation and development of effective countermeasures. *Life Sci Space Res (Amst)*. 2014;1(1):10-43. doi:10.1016/j.lssr.2014.02.004
17. Straume T. Space Radiation Effects on Crew During and After Deep Space Missions. *Curr Pathobiol Rep*. 2018;6(3):167-175. doi:10.1007/s40139-018-0175-9
18. Kennedy AR. Biological effects of space radiation and development of effective countermeasures. *Life Sci Space Res (Amst)*. 2014;1(1):10-43. doi:10.1016/j.lssr.2014.02.004
19. Cucinotta FA, Alp M, Sulzman FM, Wang M. Space radiation risks to the central nervous system. *Life Sci Space Res (Amst)*. 2014;2:54-69. doi:10.1016/j.lssr.2014.06.003
20. Talapko J, Talapko D, Katalinić D, et al. Health Effects of Ionizing Radiation on the Human Body. *Medicina (Lithuania)*. 2024;60(4). doi:10.3390/medicina60040653
21. Willey JS, Britten RA, Blaber E, et al. The individual and combined effects of spaceflight radiation and microgravity on biologic systems and functional outcomes. *J Environ Sci Health C Toxicol Carcinog*. 2021;39(2):129-179. doi:10.1080/26896583.2021.1885283
22. Mao XW, Pecaute MJ, Gridley DS. Acute Risks of Space Radiation. In: *Handbook of Bioastronautics*. Springer International Publishing; 2021:263-276. doi:10.1007/978-3-319-12191-8_27
23. Furukawa S, Nagamatsu A, Neno M, et al. Space Radiation Biology for “Living in Space.” *Biomed Res Int*. 2020;2020. doi:10.1155/2020/4703286
24. Marfia G, Navone SE, Guarnaccia L, et al. Space flight and central nervous system: Friends or enemies? Challenges and opportunities for neuroscience and neuro-oncology. *J Neurosci Res*. 2022;100(9):1649-1663. doi:10.1002/jnr.25066
25. Romero E, Francisco D. The NASA human system risk mitigation process for space exploration. *Acta Astronaut*. 2020;175:606-615. doi:10.1016/j.actaastro.2020.04.046
26. Rabbany SY, Rooney DM, Merna N. Mechanics of the Musculoskeletal System. In: Rabbany SY, Rooney DM, Merna N, eds. *Fundamentals of Biomechanics: From Cells to Organ Systems*. Springer Nature Switzerland; 2024:109-142. doi:10.1007/978-3-031-71522-8_4
27. Potoupnis M, Yavropoulou MP. The role of mechanical factors on the musculoskeletal system. Published online 2017. doi:10.1016/j
28. Bergman S. Public health perspective - how to improve the musculoskeletal health of the population. *Best Pract Res Clin Rheumatol*. 2007;21(1):191-204. doi:10.1016/j.berh.2006.08.012
29. Kell RT, Bell G, Quinney A. *Musculoskeletal Fitness, Health Outcomes and Quality of Life*.
30. Powers JD, Malingen SA, Regnier M, Daniel TL. The Sliding Filament Theory Since Andrew Huxley: Multiscale and Multidisciplinary Muscle Research. *Annual Review of*

- Biophysics* Downloaded from www.annualreviews.org Guest. 2024;39:58.
doi:10.1146/annurev-biophys-110320
31. Craig R, Padrón R, Craig RW. *Chapter 7 Molecular Structure of the Sarcomere Molecular Structure of the Sarcomere Molecular Structure of the Sarcomere Introduction Structure and Function of Striated Muscle.*; 2004.
<https://www.researchgate.net/publication/256326303>
 32. Karp JR. *Muscle Fiber Types and Training*. Vol 21.; 2001.
<http://journals.lww.com/nsca-scj>
 33. Talmadge RJ, Roy RR, Edgerton R V. muscle_fiber_types_and_function.2. *Curr Opin Rheumatol*. 1993;5(5(6)):695-705.
 34. Bloemberg D, Quadrilatero J. Rapid determination of myosin heavy chain expression in rat, mouse, and human skeletal muscle using multicolor immunofluorescence analysis. *PLoS One*. 2012;7(4). doi:10.1371/journal.pone.0035273
 35. Schiaffino S. Fibre types in skeletal muscle: A personal account. *Acta Physiologica*. 2010;199(4):451-463. doi:10.1111/j.1748-1716.2010.02130.x
 36. Bagley JR, Murach K. *Microgravity-Induced Fiber Type Shift in Human Skeletal Muscle.*; 2012. <https://www.researchgate.net/publication/264083675>
 37. Trappe S, Costill D, Gallagher P, et al. Exercise in space: human skeletal muscle after 6 months aboard the International Space Station. *J Appl Physiol*. 2009;106:1159-1168. doi:10.1152/jappphysiol.91578.2008.-The
 38. Fitts RH, Trappe SW, Costill DL, et al. Prolonged space flight-induced alterations in the structure and function of human skeletal muscle fibres. *Journal of Physiology*. 2010;588(18):3567-3592. doi:10.1113/jphysiol.2010.188508
 39. Tanaka K, Nishimura N, Kawai Y. Adaptation to microgravity, deconditioning, and countermeasures. *Journal of Physiological Sciences*. 2017;67(2):271-281.
doi:10.1007/s12576-016-0514-8
 40. Chen B, Shan T. The role of satellite and other functional cell types in muscle repair and regeneration. *J Muscle Res Cell Motil*. 2019;40(1). doi:10.1007/s10974-019-09511-3
 41. Bazgir B, Fathi R, Valojerdi MR, Mozdziak P, Asgari A. *Satellite Cells Contribution to Exercise Mediated Muscle Hypertrophy and Repair Citation: Bazgir B, Fathi R, Rezazadeh Valojerdi M, Mozdziak P, Asgari AR. Satellite Cells Contribution to Exercise Mediated Muscle Hypertrophy and Repair*. Vol 18.
 42. Tedesco FS, Dellavalle A, Diaz-Manera J, Messina G, Cossu G. Repairing skeletal muscle: Regenerative potential of skeletal muscle stem cells. *Journal of Clinical Investigation*. 2010;120(1):11-19. doi:10.1172/JCI40373
 43. Sousa-Victor P, García-Prat L, Muñoz-Cánoves P. Control of satellite cell function in muscle regeneration and its disruption in ageing. *Nat Rev Mol Cell Biol*. 2022;23(3):204-226. doi:10.1038/s41580-021-00421-2
 44. Masuda S, Hisamatsu T, Seko D, et al. Time- and dose-dependent effects of total-body ionizing radiation on muscle stem cells. *Physiol Rep*. 2015;3(4).
doi:10.14814/phy2.12377
 45. Jurdana M. Radiation effects on skeletal muscle. *Radiol Oncol*. 2008;42(1):15-22.
doi:10.2478/v10019-007-0034-5

46. Jurdana M, Cemazar M, Pegan K, Mars T. Effect of ionizing radiation on human skeletal muscle precursor cells. In: *Radiology and Oncology*. Vol 47. Sciendo; 2013:376-381. doi:10.2478/raon-2013-0058
47. Juban G, Chazaud B. Metabolic regulation of macrophages during tissue repair: insights from skeletal muscle regeneration. *FEBS Lett*. 2017;591(19):3007-3021. doi:10.1002/1873-3468.12703
48. Kharraz Y, Guerra J, Mann CJ, Serrano AL, Muñoz-Cánoves P. Macrophage plasticity and the role of inflammation in skeletal muscle repair. *Mediators Inflamm*. 2013;2013. doi:10.1155/2013/491497
49. Chazaud B. Inflammation and Skeletal Muscle Regeneration: Leave It to the Macrophages! *Trends Immunol*. 2020;41(6):481-492. doi:10.1016/j.it.2020.04.006
50. Chazaud B, Brigitte M, Yacoub-Youssef H, et al. *Dual and Beneficial Roles of Macrophages During Skeletal Muscle Regeneration*. Vol 37.; 2009. www.acsm-essr.org
51. Caiozzo VJ, Giedzinski E, Baker M, et al. The radiosensitivity of satellite cells: Cell cycle regulation, apoptosis and oxidative stress. *Radiat Res*. 2010;174(5):582-589. doi:10.1667/RR2190.1
52. Viana W, Lambertz D, Borges E, Melo J, Lambertz K, Amaral A. Late Effects of Radiation on Skeletal Muscle: An Open Field of Research. *J Biomed Sci Eng*. 2015;08(08):555-570. doi:10.4236/jbise.2015.88052
53. McDonald AA, Kunz MD, McLoon LK. Dystrophic changes in extraocular muscles after gamma irradiation in mdx:utrophin+/- mice. *PLoS One*. 2014;9(1). doi:10.1371/journal.pone.0086424
54. Hardee JP, Puppa MJ, Fix DK, et al. The effect of radiation dose on mouse skeletal muscle remodeling. *Radiol Oncol*. 2014;48(3):247-256. doi:10.2478/raon-2014-0025
55. Bandstra ER, Thompson RW, Nelson GA, et al. Musculoskeletal changes in mice from 2050 cGy of simulated galactic cosmic rays. *Radiat Res*. 2009;172(1):21-29. doi:10.1667/RR1509.1
56. Zhou Y, Sheng X, Deng F, et al. Radiation-induced muscle fibrosis rat model: Establishment and valuation. *Radiation Oncology*. 2018;13(1). doi:10.1186/s13014-018-1104-0
57. Phillips SM, Tipton KD, Ferrando AA, Wolfe RR. *Resistance Training Reduces the Acute Exercise-Induced Increase in Muscle Protein Turnover*.; 1999.
58. Picosky MA, Gaine PC, Martin WF, et al. *Nutrient Physiology, Metabolism, and Nutrient-Nutrient Interactions Aerobic Exercise Training Increases Skeletal Muscle Protein Turnover in Healthy Adults at Rest 1,2*. Vol 17.; 2003.
59. Bazgir B, Fathi R, Valojerdi MR, Mozdziak P, Asgari A. *Satellite Cells Contribution to Exercise Mediated Muscle Hypertrophy and Repair Citation: Bazgir B, Fathi R, Rezazadeh Valojerdi M, Mozdziak P, Asgari AR. Satellite Cells Contribution to Exercise Mediated Muscle Hypertrophy and Repair*. Vol 18.
60. Scott JM, Feiveson AH, English KL, et al. Effects of exercise countermeasures on multisystem function in long duration spaceflight astronauts. *NPJ Microgravity*. 2023;9(1). doi:10.1038/s41526-023-00256-5

61. English KL, Downs M, Goetchius E, et al. High intensity training during spaceflight: results from the NASA Sprint Study. *NPJ Microgravity*. 2020;6(1). doi:10.1038/s41526-020-00111-x
62. Fujino H, Ishihara A, Murakami S, et al. Protective effects of exercise preconditioning on hindlimb unloading-induced atrophy of rat soleus muscle. *Acta Physiologica*. 2009;197(1):65-74. doi:10.1111/j.1748-1716.2009.01984.x
63. Hurst JE, Fitts RH. Hindlimb unloading-induced muscle atrophy and loss of function: Protective effect of isometric exercise. *J Appl Physiol*. 2003;95(4):1405-1417. doi:10.1152/jappphysiol.00516.2002
64. Naito M, Kodaira S, Ogawara R, et al. Investigation of shielding material properties for effective space radiation protection. *Life Sci Space Res (Amst)*. 2020;26:69-76. doi:10.1016/j.lssr.2020.05.001
65. Montesinos CA, Khalid R, Cristea O, et al. Space radiation protection countermeasures in microgravity and planetary exploration. *Life*. 2021;11(8). doi:10.3390/life11080829
66. Lemon JA, Boreham DR, Rollo CD. *A Dietary Supplement Abolishes Age-Related Cognitive Decline in Transgenic Mice Expressing Elevated Free Radical Processes*. Vol 228.; 2003.
67. Lemon JA, Boreham DR, David Rollo C. *A Complex Dietary Supplement Extends Longevity of Mice*.; 2005. <http://biomedgerontology.oxfordjournals.org/>
68. Lemon JA, Rollo CD, Boreham DR. Elevated DNA damage in a mouse model of oxidative stress: Impacts of ionizing radiation and a protective dietary supplement. *Mutagenesis*. 2008;23(6):473-482. doi:10.1093/mutage/gen036
69. Lemon JA, Aksenov V, Samigullina R, et al. A multi-ingredient dietary supplement abolishes large-scale brain cell loss, improves sensory function, and prevents neuronal atrophy in aging mice. *Environ Mol Mutagen*. 2016;57(5):382-404. doi:10.1002/em.22019
70. Hutton CP, Lemon JA, Sakic B, et al. Early intervention with a multi-ingredient dietary supplement improves mood and spatial memory in a triple transgenic mouse model of Alzheimer's disease. *Journal of Alzheimer's Disease*. 2018;64(3):835-857. doi:10.3233/JAD-170921
71. Hughes MC, Ramos S V., Turnbull PC, et al. Early myopathy in Duchenne muscular dystrophy is associated with elevated mitochondrial H₂O₂ emission during impaired oxidative phosphorylation. *J Cachexia Sarcopenia Muscle*. 2019;10(3):643-661. doi:10.1002/jcsm.12405
72. Zhou T, Lu L, Wu S, Zuo L. Effects of ionizing irradiation on mouse diaphragmatic skeletal muscle. *Front Physiol*. 2017;8(JUL). doi:10.3389/fphys.2017.00506
73. De Lisio M, Kaczor JJ, Phan N, Tarnopolsky MA, Boreham DR, Parise G. Exercise training enhances the skeletal muscle response to radiation-induced oxidative stress. *Muscle Nerve*. 2011;43(1):58-64. doi:10.1002/mus.21797
74. Patel ZS, Brunstetter TJ, Tarver WJ, et al. Red risks for a journey to the red planet: The highest priority human health risks for a mission to Mars. *NPJ Microgravity*. 2020;6(1). doi:10.1038/S41526-020-00124-6

75. Dartnell LR. Ionizing radiation and life. *Astrobiology*. 2011;11(6):551-582. doi:10.1089/ast.2010.0528
76. Hellweg CE, Baumstark-Khan C. Getting ready for the manned mission to Mars: The astronauts' risk from space radiation. *Naturwissenschaften*. 2007;94(7):517-526. doi:10.1007/s00114-006-0204-0
77. Donaubaue AJ, Deloch L, Becker I, Fietkau R, Frey B, Gaip US. The influence of radiation on bone and bone cells—differential effects on osteoclasts and osteoblasts. *Int J Mol Sci*. 2020;21(17):1-19. doi:10.3390/ijms21176377
78. Scott BR. Low-Dose Radiation-Induced Protective Process and Implications for Risk Assessment, Cancer Prevention, and Cancer Therapy. *Dose-Response*. 2007;5(2):dose-response.0. doi:10.2203/dose-response.05-037.scott
79. Sazykina TG. Population sensitivities of animals to chronic ionizing radiation-model predictions from mice to elephant. *J Environ Radioact*. 2018;182:177-182. doi:10.1016/j.jenvrad.2017.11.013
80. Sihver L, Mortazavi S. 2019 *IEEE Aerospace Conference*. IEEE; 2019.
81. Chaturvedi A, Jain V. Effect of Ionizing Radiation on Human Health. *INTERNATIONAL JOURNAL OF PLANT AND ENVIRONMENT*. 2019;5(03):200-205. doi:10.18811/ijpen.v5i03.8
82. Powers SK, Radak Z, Ji LL, Jackson M. Reactive oxygen species promote endurance exercise-induced adaptations in skeletal muscles. *J Sport Health Sci*. 2024;13(6):780-792. doi:10.1016/j.jshs.2024.05.001
83. Chen MM, Li Y, Deng SL, Zhao Y, Lian ZX, Yu K. Mitochondrial Function and Reactive Oxygen/Nitrogen Species in Skeletal Muscle. *Front Cell Dev Biol*. 2022;10. doi:10.3389/fcell.2022.826981
84. Klement RJ, Champ CE. Calories, carbohydrates, and cancer therapy with radiation: Exploiting the five R's through dietary manipulation. *Cancer and Metastasis Reviews*. 2014;33(1):217-229. doi:10.1007/s10555-014-9495-3
85. Lin YH, Chang KP, Lin YS, Chang TS. Evaluation of effect of body mass index and weight loss on survival of patients with nasopharyngeal carcinoma treated with intensity-modulated radiation therapy. *Radiation Oncology*. 2015;10(1). doi:10.1186/s13014-015-0443-3
86. Stein TP. Weight, muscle and bone loss during space flight: Another perspective. *Eur J Appl Physiol*. 2013;113(9):2171-2181. doi:10.1007/s00421-012-2548-9
87. Lee PHU, Chung M, Ren Z, Mair DB, Kim DH. Factors mediating spaceflight-induced skeletal muscle atrophy. *Am J Physiol Cell Physiol*. 2022;322(3):C567-C580. doi:10.1152/ajpcell.00203.2021
88. Collao N, D'Souza D, Messeiller L, et al. Radiation induces long-term muscle fibrosis and promotes a fibrotic phenotype in fibro-adipogenic progenitors. *J Cachexia Sarcopenia Muscle*. 2023;14(5):2335-2349. doi:10.1002/jcsm.13320
89. Fajardo LF. The pathology of ionizing radiation as defined by morphologic patterns. In: *Acta Oncologica*. Vol 44. ; 2005:13-22. doi:10.1080/02841860510007440
90. Allam O, Park KE, Chandler L, et al. The impact of radiation on lymphedema: A review of the literature. *Gland Surg*. 2020;9(2):596-602. doi:10.21037/g.2020.03.20

91. Chowdhury P, Akel N, Jamshidi-Parsian A, et al. *Degenerative Tissue Responses to Space-like Radiation Doses in a Rodent Model of Simulated Microgravity.*; 2016. www.annclinlabsci.org
92. O'Connor TN, Kallenbach JG, Orciuoli HM, et al. Endurance exercise attenuates juvenile irradiation-induced skeletal muscle functional decline and mitochondrial stress. *Skelet Muscle*. 2022;12(1). doi:10.1186/s13395-022-00291-y
93. Bandstra ER, Thompson RW, Nelson GA, et al. Musculoskeletal Changes in Mice from 20–50 cGy of Simulated Galactic Cosmic Rays. *Radiat Res*. 2009;172(1):21-29. doi:10.1667/RR1509.1
94. Anderson EJ, Neufer PD. Type II skeletal myofibers possess unique properties that potentiate mitochondrial H₂O₂ generation. *Am J Physiol Cell Physiol*. 2006;290(3). doi:10.1152/ajpcell.00402.2005
95. De Lisio M, Kaczor JJ, Phan N, Tarnopolsky MA, Boreham DR, Parise G. Exercise training enhances the skeletal muscle response to radiation-induced oxidative stress. *Muscle Nerve*. 2011;43(1):58-64. doi:10.1002/mus.21797
96. Leeuwenburgh C, Hollander J, Leichtweis S, et al. *Adaptations of Glutathione Antioxidant System to Endurance Training Are Tissue and Muscle Fiber Specific.*
97. Wang X, Zhou L. The Many Roles of Macrophages in Skeletal Muscle Injury and Repair. *Front Cell Dev Biol*. 2022;10. doi:10.3389/fcell.2022.952249
98. Emanuelsson EB, Baselet B, Neefs M, et al. Myeloid cell infiltration in skeletal muscle after combined hindlimb unloading and radiation exposure in mice. *NPJ Microgravity*. 2023;9(1). doi:10.1038/s41526-023-00289-w
99. Millet GY, Martin V, Martin A, Vergès S. Electrical stimulation for testing neuromuscular function: From sport to pathology. *Eur J Appl Physiol*. 2011;111(10):2489-2500. doi:10.1007/s00421-011-1996-y
100. Doucet BM, Lam A, Griffin L. *FoCUS: BioMEDICAL ENGINEERING Neuromuscular Electrical Stimulation for Skeletal Muscle Function*. Vol 85.; 2012.
101. Khosla S, Oursler MJ, Monroe DG. Estrogen and the skeleton. *Trends in Endocrinology and Metabolism*. 2012;23(11):576-581. doi:10.1016/j.tem.2012.03.008
102. Vanderschueren D, Vandenput L, Boonen S, Lindberg MK, Bouillon R, Ohlsson C. Androgens and bone. *Endocr Rev*. 2004;25(3):389-425. doi:10.1210/er.2003-0003
103. Kitajima Y, Ono Y. Estrogens maintain skeletal muscle and satellite cell functions. *Journal of Endocrinology*. 2016;229(3):267-275. doi:10.1530/JOE-15-0476
104. Burke M, Wong K, Talyansky Y, et al. Sexual dimorphism during integrative endocrine and immune responses to ionizing radiation in mice. *Sci Rep*. 2024;14(1). doi:10.1038/s41598-023-33629-7
105. Mark S, Scott GBI, Donoviel DB, et al. The impact of sex and gender on adaptation to space: Executive summary. *J Womens Health*. 2014;23(11):941-947. doi:10.1089/jwh.2014.4914